Multi-Scale Detection and Characterization of Physical and Ecological Change in the Arctic Using Satellite Remote Sensing

by

Liza Kay Jenkins

A dissertation submitted in partial fulfillment
of the requirements for the degree of
Doctor of Philosophy
(Environment and Sustainability)
in The University of Michigan
2019

Doctoral Committee:

Professor William S. Currie, Chair
Adjunct Professor Nancy H.F. French, Michigan Technological University
Professor Guy A. Meadows
Adjunct Professor Robert A. Shuchman, Michigan Technological University
Professor Michael J. Wiley

Liza Kay Jenkins

lliverse@umich.edu

ORCID iD: 0000-0002-8309-5396

DEDICATION

This dissertation is dedicated to the next generation – especially my children

Mackenzie Kay Jenkins and Calder Michael Jenkins.

ACKNOWLEDGEMENTS

This work was supported in party by NASA Terrestrial Ecology Grants # NNX15AT79A, #NNX10AF41G, and #NNX13AK44G and the Conservation of Arctic Flora and Fauna (CAFF), Biodiversity Working Group of the Arctic Council, Advancement of the Arctic Land Cover Initiative through Applied Remote Sensing Award No: CAFF PROJECT NO. 000060.

I would like to acknowledge my dissertation committee for all their help guiding the research design, implementation, analysis, and writing of this dissertation. I would especially like to thank my Committee Chair, Dr. Currie, for believing in me and pushing me to be a better scholar and scientist.

I would also like to thank my co-authors of the published version of Chapter II: Laura Bourgeau-Chavez, Nancy French, Tatiana Loboda, and Brian Thelen; and the in-press version of Chapter III: Tom Barry, Karl Bosse, William Currie, Tom Christensen, Sara Longan, Robert Shuchman, Danielle Tanzer, and Jason Taylor.

The work in Chapter IV wouldn't have been possible without the tough humans that worked as the field crews for the NASA ABoVE Tundra Fire Project: Tatiana Loboda, Dong (Tony) Chen, Andrew Poley, Jiaying He, Garrett Jones, and Jon Hirsh. Thank you for the endless weeks of adventure and teamwork in the soggy tundra tripping over tussocks. Thank you to Laura Bourgeau-Chavez, Karl Bosse, and Andew Poley for their help in developing tundra-specific soil

moisture calibration coefficients and post-field work processing of soil samples. Thank you to the previous NASA tundra fire projects and scientists, and the NASA ABoVE Science Team, that helped developed field protocols that were modified for the project.

Thank you to my employer, Michigan Technological University. A special thank you to my department, the Michigan Tech Research Institute (MTRI), and MTRI Co-Director, Bob Shuchman. Thank you for your flexibility in allowing me to continue my education while working and for providing resources to make the process easier.

Thank you to my lifelong teammate, Chris Jenkins, and our beautiful children, Mackenzie and Calder, that push me to do more to make the world better. Thank you to my entire family and especially my mom, Jackie Liversedge, and sister, Lacy Muhich, for their lifelong support.

TABLE OF CONTENTS

LIST OF FIGURES

LIST OF TABLES

ABSTRACT

The Arctic environment is in a state of transition as the result of climate warming. There are tremendous implications for ecology, human well-being, national security, and energy and economic development among many other critical issues. The effects of Arctic warming are multifarious. Both physical and ecological processes have been affected in a set of complex feedback mechanisms.

The objective of this dissertation research is to develop new technology though advanced computing and improved data availability to identify environmental baselines and trends. This is accomplished through the use of different satellite remote sensing platforms at different spatial and temporal scales. This research provides needed methods and baseline data and identifies temporal trends for environmental monitoring programs in the Arctic. Among other uses, the data presented here will allow future evaluation of continued change and disturbance.

Using electro-optical satellite data spanning the pan-Arctic, and standardizing in terms of data and satellite platform, an unbiased comparison across numerous disparate variables and across terrestrial and marine environments provides a method to detect and evaluate environmental change. Using MODIS standard products of land surface temperature, percent snow covered area, NDVI, EVI, phenology, burned area, marine chlorophyll, CDOM, sea surface temperature, and marine primary productivity, time series data 2000-2017 shows significant

temporal trends in almost all variables. Analysis of seasonal data reveals significant breakpoints in temporal trends over the 18-year period. Within the terrestrial environment, data shows significant increasing trends in land surface temperature and NDVI. In the marine environment, significant increasing trends are detected in primary productivity. Significantly earlier onset of greenup date and longer end of growing season are observed in certain bioclimate subzones. Terrestrial and marine observations show similar rates of change with unidirectional change in terrestrial and significant directional and magnitude shifts in marine.

There is great potential to use a specific type of active remote sensing, Synthetic Aperture Radar (SAR), for Arctic change detection and disturbance monitoring due to its all-weather imaging capabilities and the ability for SAR to provide information on vegetation structure, biomass, and moisture conditions. In contrast to electro-optical studies from the same region, measures of landscape recovery to pre-burn conditions, as detected by SAR, are on the order of four to five years instead of one. A 3 dB difference exists between burned and unburned tundra, with the best time for burned area detection being late in the growing season before frozen ground conditions develop. Models developed using in-situ field data in burned and unburned areas of the tundra show SAR backscatter is a function of moisture condition, shrubs, tussocks, and fire. Contributions of different biophysical variables to the backscatter signal vary as a result of year since fire, but models show contributions from all four categories in almost all fire histories.

Advanced methods to look at synoptic change at a variety of scales are needed to increase our understanding of this remote environment and provide a baseline status upon

which to evaluate change. This dissertation works toward the development of methods and datasets for change evaluation.

Chapter I

Introduction: Arctic Change and the Need for Advanced Analysis Methods

Climate Change and the Arctic Environment

The Arctic is particularly sensitive to climate change, and northern high latitudes have been identified as a region where climate change effects will be stronger and happen earlier than other regions of the world (Chapin et al. 2000, Serreze et al. 2000, Hinzman et al. 2005). Arctic meteorological records indicate that air temperatures have generally increased across the Arctic since the end of the Little Ice Age (~1870). Paleoclimate records from lake sediments, trees, glaciers, and marine sediments show the highest temperatures over the last four centuries were from the mid-1980s to the mid-20th century (Overpeck et al. 1997). Much of the Arctic did experience a cooling trend between 1940 and 1970, but a pronounced warming trend has been observed since the 1970s. Overall warming in the 19th to 20th centuries was 1° to 3°C locally and 1.5° C averaged over the Arctic (Jacoby and D'Arrigo 1989, Jones and Bradley 1992, Lamoureux and Bradley 1996, Briffa et al. 1996, Garfinkel and Brubaker 1980, Lachenbruch and Marshall 1986, Kakuta 1992, Beltrami and Taylor 1995, Calkin 1988, Wiles 1991, Caseldine and Stötter 1993, Szeicz and MacDonald 1995, Evison 1996).

Difficulties arise when comparing climate trends across different regions in the pan-Arctic due to sparse and inconsistent instrumentation. Few temperature records longer than 100 years exist. One consistent issue among various studies is the marked differences observed in regional climate trends. In the latter half of the 20th century Western North America has experienced strong warming trends while Eastern Canada and Siberia have experienced little change and even slight cooling in some locations (ACIA, 2004).

A variety of other changes beyond increased air temperature have been observed within the Arctic system over the past 400 years with many of these changes initiated or accelerated coincident with the marked increase in warming that occurred in the 1970s (Overpeck et al. 1997). Evidence from terrestrial, marine, and atmospheric studies all indicate that the overall climate of the Arctic has changed significantly since the 1970s (Hinzman et al. 2005). Evidence includes: more variable and less predictable weather; more frequent 2-4°C warming and thawing of permafrost; decrease in size of thermokarst lakes; increasing rates of coastal erosion; increase in river base flow; earlier lake and river breakup and delayed freeze-up; increased lake water temperature and alkalinity; decline in in precipitation and precipitation minus potential evapotranspiration (P-PET); thinning, recession, and reduced mass of ice caps and glaciers; earlier snowmelt; increased shrub abundance and other vegetation change; tree line advancing northward; and tundra carbon flux change from sink to source to the atmosphere. Many of these, like temperature, serve as both indicators and drivers of change in the Arctic. Additionally, the effects of climate change are amplified in the Arctic due to a variety of positive feedback mechanisms (ACIA 2004).

The effects of a warming climate are initially expected to be evident in atmospheric and near-surface processes. As additional heat fluxes are added to the Arctic, either directly through increased air temperatures or longer ice-free periods and indirectly though modified surface reflectance, these fluxes will move from the atmosphere to the land and be transferred downward through the soil profile. Later effects of climate change will be expressed in geomorphological evolution and hydrological response to changes in permafrost. It is expected that the broadest impacts to the terrestrial Arctic will be the result of climate-driven changes to the distribution and dynamics of permafrost (Hinzman et al. 2005).

The thickness of the active layer, or depth of seasonal permafrost thaw, is driven primary by surface temperature and length of the growing season. Vegetation cover, thermal properties of the surface and substrate, soil moisture, and modes of heat transfer also affect the active layer thickness (Hinkel et al. 1997, Paetzold et al. 2000, Brown et al. 2000, Kane et al. 2001, Walker et al. 2003). A significant number of studies have shown evidence of permafrost warming and thawing across Arctic Alaska. Lachenbrush and Marshall (1986) showed a 2-4°C increase over the last 50-100 years on the North Slope of Alaska and Clow and Urban (2002) showed a similar ~3°C warming since the late 1980s on the North Slope Coastal Plain and Brooks Range Foothills. Osterkamp (2003) published data from five wells at 20m depth in a north-south gradient from Prudhoe Bay to the Brooks Range. These data show broad scale warming, with some years of cooling, over the past 25 years. Modelling efforts by Romanovsky and Osterkamp (2000) at Barrow, Alaska showed cooling from 1950-1970 followed by warming, mimicking the surface air temperature trends. Further, a similar 2-3°C warming was measured at Prudhoe Bay, Alaska by Romanovsky and Osterkamp (1997) and Osterkamp (2003).

Thermokarst lakes are a sign of local permafrost degradation. Degraded permafrost can result in the gradual or catastrophic drainage of lakes (Yoshikawa and Hinzman 2003). Lake area change and complete lake drying has also been observed in non-thermokarst lakes in the high Arctic (Smol and Douglas 2007). These lakes are not influenced by permafrost and represent a more direct link to atmospheric variables such as temperature and precipitation. Other physical and chemical changes are also occurring in Arctic lakes including increase in water temperatures and increased alkalinity (Hobbie et al. 2003).

Increased future temperatures are expected to alter the phase of precipitation, the length of the melt season, the distribution of permafrost, and the depth of the active layer. These are all expected to affect overall water distribution in the Arctic. There are large uncertainties is present-day quantification of precipitation and evaporation throughout the Arctic. Given these uncertainties, quantification of variations and trends in precipitation and evaporation is limited. Even so, the Intergovernmental Panel on Climate Change (IPCC 1996, IPCC 2001) has consistently reported 20th-century precipitation increases in northern high latitudes.

The projected increases in P-PET imply an increase in water availability across the terrestrial system. Specifically, this means wetter soils when not frozen, increased surface flows in the active layer and greater ice content in the upper soil layer in the winter (ACIA 2004). Projected increases in evaporation during the summer raises the possibility that P-PET could decrease resulting in a relative drying of soils during the warm season. Indeed, recent trends of increased evaporation have been measured in the Yenisey and Mackenzie Basins (ACIA 2004).

Soil moisture dynamics are complicated and will depend on the location, timing, and amount of precipitation, changes to evaporation, permafrost melting, local climate factors, and geographic position. Soil moisture is expected to increase across the Arctic but some areas may also experience localized drying. There are no long term records of soil moisture in the Arctic but changes in water availability can be estimated from surface water balance calculations. P-PET has declined significantly in Arctic Alaska since the 1960s in both interior North Slope sites and sites along the coast of the North Slope (Hinzman et al. 2005). Substantial interannual variation was found for P-PET but an average decrease of 2.0 mm/yr was measured at coastal sites and 5.5 mm/yr in the interior North Slope (Hinzman et al. 2005).

Shrub expansion has been observed in the Arctic and is directly attributed to temperature increases that have removed limitations to reproduction and growth (Walker 1987, Lantz et al. 2010) and indirectly to increased soil microbial activity and mobilization of limiting nutrients (Strum et al. 2005). An increase in shrubs and an associated reduction in moss and lichens could alter ecological processes in several ways. Tall shrubs trap more snow than the low-stature vegetation being replaced resulting in an increase in winter ground temperatures, microbial activity, and nutrient mineralization, all contributing to positive feedback and increased shrub growth (Sturm et al. 2005). Deeper, more insulating snow could potential reduce the growing season length, increase snow melt runoff, and increase summer soil moisture (Strum et al. 2001). In general, increased evaporative demand in the Arctic will result in increased evapotranspiration from shrubs. This will serve to move more water from the soil to the atmosphere. The role shrubs, and increasing shrub cover, plays in soil moisture dynamics is complex and needs to be investigated further.

Arctic Tundra Fire and Effects on Carbon Stocks and Ecosystem Functioning

Wildfire can rapidly transfer large stocks of terrestrial carbon (C) to the atmosphere through combustion of organic material and emissions to the atmosphere. Fire oxidizes organic C primarily to, but also releases smaller quantities of CH_4, carbon monoxide, and other volatile C compounds. Carbon emissions from fire depend on pre-fire biomass, soil organic matter, bulk density, and depth of burn (Abbott et al.). Despite the low-biomass areas of the tundra, wildfires in the Arctic have the potential to significantly affect global carbon storage because significant carbon stocks are also present in the soil and fire can initiate a set of positive feedback mechanisms to climate warming.

Wildfires burn approximately 4,200 km^2 per year in the tundra with 8 TgC per year in emissions (Abbott et al., upscale from Rocha et al., 2012 and Mach et al., 2011). There are considerable uncertainties in these estimates. The soil organic carbon (SOC) pool over the entire Arctic domain is estimated to be 496 PgC (Tarnocai et al. 2009). A robust study by Ping et al. (2008) with extensive in-situ samples estimates the North American Arctic SOC pool to be 98.2 Gt with 19.2 Gt in the surface layer, 42.1 Gt in the subsurface active layer, and 36.9 in the permafrost. These estimates show that approximately 19.6% of the 1 meter depth SOC stores in the Arctic are susceptible to loss through fire because it is contained in the surface organic horizons (Ping et al. 2008).

The amount of C released from tundra fires is variable and largely dependent on fire size and severity. Most tundra fires are small (French et al. 2015) and relatively unstudied. The 2007

Anaktuvuk River Fire was unprecedented in terms of both fire characteristics for the region and focus of scientific study. This large, severe, late-season fire released approximately 2.1 TgC to the atmosphere (Mack et al. 2011). This is roughly equivalent to the annual net C sink for the entire Arctic biome averaged over the last quarter of the twentieth century (Mack et al. 2011). 62 +/- 4% of the 2.1 TgC release was from SOC with the remainder from plant biomass. This fire was unique in terms of modern fire history for the region, but has served to provide needed study and baseline data of fire in the Arctic. The Anaktuvuk River Fire also underscores the potential for significant change in carbon cycling from fire and changing fire regime in the tundra.

Wildfire is a climate-sensitive process. Measurements from the Anaktuvuk River Fire show the upward potential for large quantities of C release from a large and severe tundra fire. Recent observations indicate increased burned area in the tundra over the past two decades (Higuera et al. 2008, Hu et al. 2010). Given changes in climate, tundra fires could become both more frequent and severe in the future (Hu et al. 2010). Increasing fire in the Arctic could rapidly transfer large amounts of C to the atmosphere, reduce landscape C storage, and amplify climate warming through increased levels and post-fire changes to the ecosystem.

Wildfire in the Arctic can significantly change land surface biophysical properties, post-fire surface energy exchange, and surface temperature. Post-fire changes to the ecosystem can expose additional SOC stores beyond the initial combustion of the organic surface layer and further affect ecosystem C balance. Surface reflectance is altered post-fire with a decrease in albedo (Liljedahl et al. 2007, Mack et al. 2011, Rocha and Shaver 2011). Tundra vegetation is more reflective than recently burned ground and surface darkening from charred vegetation

has been shown to result in increased soil temperatures at burned sites (Liljedahl et al. 2007, Rocha and Shaver 2009). Differences in measured surface energy have been shown to be a function of burn severity with severely burned tundra having lower albedo and higher net radiation than moderately or unburned tundra (Rocha and Shaver 2011a). Vegetation regrowth leads to rapid recovery of albedo, but fundamental changes to ecosystem energy partitioning are the result of changes to organic layer depth and moss cover (Rocha and Shaver 2011a).

Fire removes the insulating layer of vegetation on the surface which effects heat transfer and storage. Latent effects resulting from the removal of the insulating upper layer of organic soil has implications for surface hydrology, soil moisture, active layer depth, and permafrost dynamics. Deeper and warmer soils have been observed in recently burned areas in the tundra as well as more rapid freezing of the soil in the fall (Rocha and Shaver 2011a). Warmer soils during the summer can lead to permafrost destabilization and increased microbial decomposition. Significant C stores exist in the lower soil profile (Ping et al. 2008) and both direct and indirect fire-induced warming can potentially release previously locked stores of C.

The vegetation community structure changes post fire (Racine et al. 2004). These vegetation changes affect both C sequestrations of the remnant and regrowth vegetation as well as the surface energy exchange. Post fire carbon sequestration is a function a burn severity with decreased sequestration found with increased severity which is most likely controlled by leaf area recovery and photosynthesis (Rocha and Shaver 2011b). Surface energy exchange is affected by the removal of surface vegetation and by the structure and composition of vegetation regrowth. Mosses and lichen are slower to recover post-fire and these vegetation types are especially good insulators (Rocha and Shaver 2011). In a study on the Seward

Peninsula, Alaska there was very little or no recovery of moss or fruitcose lichens 24 years post-fire (Racine et al. 2004). The same study also found an overall increase in shrubs as compared to pre-fire conditions. The shrubs were larger, more abundant, and of different species composition. Changes in the structure of tundra vegetation as a result of fire can directly affect the surface energy balance through changes in temperature, snow cover, and water (McFadden et al., 1998; Sturm et al., 2001). Successional legacies in boreal regions have been shown to influence ecosystem carbon sequestration from decades to centuries (Bond-Lamberty et al. 2004, Goulden et al. 2006, McMillan and Goulden 2008).

A variety of physical and biological factors affect fire-related carbon pools and processes. Primary factors include albedo, soil thermal regime, permafrost thaw, hydrology, and vegetation succession. More work is needed on quantification of these interrelated processes and feedback mechanisms, especially across the diverse gradients in soil moisture and vegetation found in the tundra.

The Impact of Climate Change on Arctic Disturbance Regimes

Disturbance is the perturbation of a normal state or regime. Disturbance is a normal component of the high northern latitude region, but within the context of climate change we need to understand how disturbance is changing and how vulnerable or resilient the Arctic is to these changes. Further work is also needed to define “normal” in order to separate disturbance effects from background conditions.

Disturbance can be characterized as either a press or pulse disturbance where press disturbance is relatively slow but persistent in nature and pulse disturbance is relatively rapid

and local (Grosse et al. 2011). Examples of press disturbance in the Arctic include thawing of permafrost from the surface down, and changes in hydrology or vegetation type, while wildfire and thermokarst are examples of pulse disturbance (Grosse et al. 2011). The impact of climate change on Arctic disturbance regimes is important to understand, and the spatial and temporal scale of disturbance (essentially press or pulse) dictates the tools most useful for baseline characterization and scientific inquiry.

Few long-term monitoring datasets exist in the Arctic to study change, and repeat measurements are a data gap frequently referenced. Satellite data is a resource for scientific study in this region that provides a way to measure change over time as data are available at a variety of spatial, temporal, and radiometric scales. Electro-optical satellite data provides one tool but microwave satellite data holds great potential in the Arctic due to its all-weather imaging capabilities that are not affected by cloud-cover, haze, and limited solar illumination. For my dissertation I plan to leverage the unique imaging capabilities offered by satellite data, and especially synthetic aperture radar data, to investigate landscape change in the Arctic.

Dissertation Summary

Arctic change detection and monitoring require intelligent matching of spatial, temporal, and radiometric scales to available tools and datasets. Satellite remote sensing is advantageous to use in the vast and largely uninhabited Arctic, but knowledge is needed of different satellite platforms available and how to utilize large data streams. Furthermore, understanding of in-situ conditions are required for interpretation of remote sensing data and to develop relationships between satellite data and field-based measurements.

This dissertation research focused on landscape response to press and pulse disturbance, together with methods development, to examine processes occurring at different scales. Three interrelated research topics presented used satellite remote sensing to create datasets to quantify ecosystem response and measure resilience to change. The research efforts provided needed baseline data for assessment and monitoring. State-of-the-art methods were developed to digest large amounts of satellite data to assess time-series trends and detect environmental change.

The first research topic in the dissertation was a study of Arctic change from a global or pan-Arctic perspective. Using MODIS Standard Products from circa 2002 to the present, both physical and ecological parameters were measured and evaluated over a time series. A comparison of the terrestrial and marine environments were conducted to evaluate the how these environments have changed over time in terms of both magnitude and direction. In this study, measurements of spatially-explicit indicators of change in both physical and ecological parameters showed how these responses differed in the marine and terrestrial environments.

The second research topic focused on regional landscape dynamics and measurements of change promulgated by fire disturbance. Specifically, the fire regime in the Alaskan tundra served as a focus area for the investigation and three tundra fires were selected for study. The research goal was to quantify the effect of fire on the landscape as measured using SAR satellite data and to monitor landscape recovery both within and adjacent to burned areas. The backscatter signature was monitored before, during, and after fire events using the 1992-2011 ERS-1 and 2 satellite data archive.

For the final research topic in the dissertation, in-situ field measurements were used to determine field-measured factors that most correlated with SAR satellite backscatter in the tundra. Findings from this study provided the information needed by future researchers to more effectively use SAR data as a tool for fire detection and measurement of fire effects.

The three research topics covered within the dissertation involved sets of observations conducted in different locations and scales, in order to infer processes occurring at different scales, and thus used different remote sensing solutions. The first research topic worked at the pan-Arctic scale, while research topic two investigated regional dynamics. The final research topic looked at site-scale measurements, with observations spread across the regional scale. Research topics two and three centered on fire in the Alaskan tundra, with the topic two focused on detection of fire and topic three on improved understanding of the remote sensing signal post fire. All research topics measured change from disturbance with research topic one focused on longer-term press disturbance from climate change and research topics two and three on shorter-term pulse disturbance from fire events.

Chapter II is currently in press as Jenkins et al. 2019 and Chapter III has been previously published as Jenkins et al. 2014.

References

Abbott, B.W., Rocha, A.V., Flannigan, M., Hollingsworth, T.N., Turetsky, M.R. (unknown) Net ecosystem carbon balance of the permafrost region: arctic and boreal wildfire background information. Not-published. Unknown.

Arctic Climate Impact Assessment (2004) Impacts of a Warming Arctic: Arctic Climate Impact Assessment. Cambridge University Press, Cambridge, UK.

Beltrami, H., Taylor, A. E. (1995) Records of climatic change in the Canadian Arctic: towards calibrating oxygen isotope data with geothermal data. Global and Planetary Change, 11(3), 127-138.

Bond-Lamberty, B., Wang, C. K., Gower, S.T. (2004) Net primary production and net ecosystem production of a boreal black spruce wildfire chronosequence. Global Change Biology, 10:473-487.

Briffa, K. R., Jones, P. D., Schweingruber, F. H., Karlén, W., Shiyatov, S. G. (1996) Tree-ring variables as proxy-climate indicators: problems with low-frequency signals. In Climatic variations and forcing mechanisms of the last 2000 years (pp. 9-41). Springer, Berlin, Heidelberg.

Brown, J., Hinkel, K. M., Nelson, F. E. (2000) The circumpolar active layer monitoring (CALM) program: Research designs and initial results. Polar Geogr., 24(3), 165–258.

Calkin, P. E. (1988) Holocene glaciation of Alaska (and adjoining Yukon Territory, Canada). Quaternary Science Reviews, 7(2), 159-184.

Caseldine, C., Stötter, J. (1993) Little Ice Age glaciation of Tröllaskagi peninsula, northern Iceland: climatic implications for reconstructed equilibrium line altitudes (ELAS). The Holocene, 3(4), 357-366.

Clow, G. D., Urban, F. E. (2002) Large permafrost warming in northern Alaska during the 1990's determined from GTN-P borehole temperature measurements. In AGU Fall Meeting Abstracts, vol. 1, p. 04.

Evison, L. H., Calkin, P. E., Ellis, J. M. (1996) Late-Holocene glaciation and twentieth-century retreat, northeastern Brooks Range, Alaska. The Holocene, 6(1), 17-24.

Fraser, R. H., Lantz, T. C., Olthof, I., Kokelj, S. V., Sims, R. A. (2014) Warming-induced shrub expansion and lichen decline in the Western Canadian Arctic. Ecosystems, 17(7), 1151-1168.

French, N. H. F., L. K. Jenkins, T. V. Loboda, M. Flannigan, R. Jandt, L. L. Bourgeau-Chavez, M. Whitley (2015) Fire in arctic tundra of Alaska: past fire activity, future fire potential, and

significance for land management and ecology. Int. J. Wildland Fire, http://dx.doi.org/10.1071/WF14167

Garfinkel, H. L., Brubaker, L. B. (1980) Modern climate–tree-growth relationships and climatic reconstruction in sub-Arctic Alaska.A. H. Lachenbruch et al., J. Geophys. Res., 87, 9301 (1982)

Goulden, M. L., Winston, G. C., McMillan, A. M. S., Litvak, M. E., Read, E. L., Rocha, A. V., Elliot, J. R. (2006) An eddy covariance mesonet to measure the effect of forest age on land-atmosphere exchange. Global Change Biology, 12: 2146-2162.

Higuera, P. E., Brubaker, L. B., Anderson, P. M., Brown, T. A., Kennedy, A. T., Hu, F. S. (2008) Frequent fires in ancient shrub tundra: implications of paleorecords for arctic environmental change. PLoS One, 3(3), e0001744.

Hinkel, K. M., Outcalt, S. I., Taylor, A. E. (1997) Seasonal patterns of coupled flow in the active layer at three sites in northwest North America. Can. J. Earth Sci., 34, 667–678.

Hinzman, L. D., Bettez, N. D., Bolton, W. R., Chapin, F. S., Dyurgerov, M. B., Fastie, C. L., Griffith, B., Hollister, R.D., Hope, A., Huntington, H.P., Jensen, A.M. (2005) Evidence and implications of recent climate change in northern Alaska and other arctic regions. Climatic Change, 72(3), 251-298.

Hobbie, J. E., Shaver, G., Laundre, J., Slavik, K., Deegan, L., O'Brien, J., Oberbauer, S., MacIntyre, S. (2003) Climate forcing at the arctic LTER site. Climate Variability and Ecosystem Response at Long-Term Ecological Research (LTER) Sites, Oxford University Press, New York, 74-91.

Hu, F. S., Higuera, P. E., Walsh, J. E., Chapman, W. L., Duffy, P. A., Brubaker, L. B., Chipman, M. L. (2010) Tundra burning in Alaska: linkages to climatic change and sea ice retreat. Journal of Geophysical Research: Biogeosciences (2005–2012), 115(G4).

Jenkins, L.K., Barry, T., Bosse, K., Currie, W., Christensen, T., Longan, S., Shuchman, R., Tanzer, D., Taylor, J. (2019) Satellite-based Decadal Change Assessments of Pan-Arctic Environments. AMBIO: A Journal of the Human Environment (In press).

Jenkins, L., Bourgeau-Chavez, L., French, N., Loboda, T., Thelen, B. (2014) Development of methods for detection and monitoring of fire disturbance in the Alaskan tundra using a two-decade long record of synthetic aperture radar satellite images. Remote Sensing, 6(7), 6347-6364.

Jones, K. R., R. S. Bradley (1992) in Climate Since A.D. 1500, R. S. Bradley and P. D. Jones, Eds. (Routledge, London, 1992), pp. 649–666.

Jacoby, G. C., D'Arrigo, R. D. (1995) Tree ring width and density evidence of climatic and potential forest change in Alaska. Global Biogeochemical Cycles, 9(2), 227-234.

Kakuta, S. (1992) Surface temperature history during the last 1000 years near Prudhoe Bay, Alaska: applying control theory to the inversion of borehole temperature profiles. Palaeogeogr. Palaeoclimatol. Palaeoecol. (Global Planet. Change Sect.), 98: 225- 244, 1992. R7

Kane, D. L., Hinkel, K. M., Goering, D. J., Hinzman, L. D., Outcalt, S. I. (2001) Non-conductive heat transfer associated with frozen soils. Global Planet. Change, 29(3–4), 275–292.

Lachenbruch, A. H., Marshall, B. V. (1986) Changing climate: geothermal evidence from permafrost in the Alaskan Arctic. Science, 234(4777), 689-696.

Lamoureux, S. F., Bradley, R. S. (1996) A late Holocene varved sediment record of environmental change from northern Ellesmere Island, Canada. Journal of Paleolimnology, 16(2), 239-255.

Lantz, T. C., Gergel, S. E., Kokelj, S. V. (2010) Spatial heterogeneity in the shrub tundra ecotone in the Mackenzie Delta Region, Northwest Territories: implications for Arctic environmental change. Ecosystems, 13(2), 194-204.

Liljedahl, A., Hinzman, L., Busey, R., Yoshikawa, K. (2007) Physical short-term changes after a tussock tundra fire, Seward Peninsula, Alaska. Journal of Geophysical Research: Earth Surface (2003–2012), 112(F2).

Mack, M. C., Bret-Harte, M. S., Hollingsworth, T. N., Jandt, R. R., Schuur, E. A., Shaver, G. R., Verbyla, D. L. (2011) Carbon loss from an unprecedented Arctic tundra wildfire. Nature, 475(7357), 489-492.

McFadden, J. P., Chapin III, F. S., Hollinger, D. Y. (1998) Subgrid-scale variability in the surface energy balance of arctic tundra. Journal of Geophysical Research, 103: 28947–28961.

McMillan, A. M. S., Goulden, M. L. (2008) Age-dependent variation in the biophysical properties of boreal forests. Global Biogeochemical Cycles, 22:2 GB2019.

Myers-Smith, I. H., Forbes, B. C., Wilmking, M., Hallinger, M., Lantz, T., Blok, D., Tape, K.D., Macias-Fauria, M., Sass-Klaassen, U., Lévesque, E., Boudreau, S. (2011) Shrub expansion in tundra ecosystems: dynamics, impacts and research priorities. Environmental Research Letters, 6(4), 045509.

Osterkamp, T. E. (2003) A thermal history of permafrost in Alaska. in Proceedings of the Eighth International Conference on Permafrost, 21–25 July 2003, Balkema Publishers, Zurich, Switzerland, pp. 863–868.

Overpeck, J., Hughen, K., Hardy, D., Bradley, R., Case, R., Douglas, M., Finney, B., Gajewski, K., Jacoby, G., Jennings, A., Lamoureux, S. (1997) Arctic environmental change of the last four centuries. Science, 278(5341), 1251-1256.

Paetzold, R. F., Hinkel, K. M., Nelson, F. E., Osterkamp, T. E., Ping, C. L., Romanovsky, V. E. (2000) Temperature and thermal properties of Alaskan soils. in Lal, R., Kimble, J. M., and Stewart, B. A. (eds.), Global Climate Change and Cold Regions Ecosystems, Lewis Publishers, Boca Raton, FL, pp. 223–245.

Ping, C. L., Michaelson, G. J., Jorgenson, M. T., Kimble, J. M., Epstein, H., Romanovsky, V. E., Walker, D. A. (2008) High stocks of soil organic carbon in the North American Arctic region. Nature Geoscience, 1(9), 615-619.

Racine, C., Jandt, R., Meyers, C., Dennis, J. (2004) Tundra fire and vegetation change along a hillslope on the Seward Peninsula, Alaska, USA. Arctic, Antarctic, and Alpine Research, 36(1), 1-10.

Rocha, A. V., Shaver, G. R. (2011a) Postfire energy exchange in arctic tundra: the importance and climatic implications of burn severity. Global Change Biology, 17(9), 2831-2841.

Rocha, A. V., Shaver, G. R. (2011b) Burn severity influences postfire exchange in arctic tundra. Ecological Applications, 21(2), 477-489.

Rocha, A. V., Shaver, G. R. (2009) Advantages of a two band EVI calculated from solar and photosynthetically active radiation fluxes. Agricultural and Forest Meteorology, 149(9), 1560-1563.

Romanovsky, V. E., Osterkamp, T. E. (1997) Thawing of the active layer on the coastal plain of the Alaskan Arctic. Permafrost Periglacial Process, 8(1), 1–22.

Ropars, P., Boudreau, S. (2012) Shrub expansion at the forest–tundra ecotone: spatial heterogeneity linked to local topography. Environmental Research Letters, 7(1), 015501.

Tremblay, B., Lévesque, E., Boudreau, S. (2012) Recent expansion of erect shrubs in the Low Arctic: evidence from Eastern Nunavik. Environmental Research Letters, 7(3), 035501.

Serreze, M. C., Walsh, J. E., Chapin, F. S., III, Osterkamp, T., Dyurgerov, M., Romanovsky,V., Oechel, W. C., Morison, J., Zhang, T., Barry, R. G. (2000) Observational evidence of recent change in the northern high latitude environment. Clim. Change, 46, 159–207.

Smol, J. P., Douglas, M. S. (2007) Crossing the final ecological threshold in high Arctic ponds. Proceedings of the national Academy of Sciences, 104(30), 12395-12397.

Sturm, M., Schimel J., Michaelson G., Welker J.M., Oberbauer S.F., Liston G.E., Fahnestock J., Romanovsky V.E. (2005) Winter biological processes could help convert Arctic tundra to shrub land. Bioscience, 55:17–26.

Sturm, M., Holmgren, J., McFadden, J. P., Liston, G. E., Chapin III, F. S., Racine, C. H. (2001) Snow-shrub interactions in Arctic tundra: a hypothesis with climatic implications. Journal of Climate, 14(3), 336-344.

Szeicz, J. M., MacDonald, G. M. (1995) Dendroclimatic reconstruction of summer temperatures in northwestern Canada since AD 1638 based on age-dependent modeling. Quaternary Research, 44(2), 257-266.

Tarnocai, C., Canadell, J. G., Schuur, E. A. G., Kuhry, P., Mazhitova, G., Zimov, S. (2009) Soil organic carbon pools in the northern circumpolar permafrost region. Global biogeochemical cycles, 23(2).

Walker, D. A., Jia, G. J., Epstein, H. E., Raynolds, M. K., Chapin, F. S., III, Copass, C. D., Hinzman, L.D., Kane, D., Maier, H., Michaelson, G. J., Nelson, F., Ping, C. L., Romanovsky, V. E., Shiklomanov, N., Shur, Y. (2003) Vegetation-soil-thaw-depth relationships along a Low- Arctic bioclimate gradient, Alaska: Synthesis of information from theATLAS studies. Permafrost and Periglacial Processes, 14, 103–123.

Wiles, G. C. (1991) in International Conference on the Role of Polar Regions in Global Change, G. Weller, Ed. (University of Alaska, Fairbanks, AK, 1991), pp. 617–625.

Yoshikawa, K., Hinzman, L. (2003) Shrinking thermokarst ponds and groundwater dynamics in discontinuous permafrost. Permafrost Periglacial Process, 14(2), 151–160.

Chapter II

Satellite-based Decadal Change Assessments of Pan-Arctic Environments[1]

Abstract

Remote sensing can advance the work of the Circumpolar Biodiversity Monitoring Program through monitoring of satellite-derived terrestrial and marine physical and ecological variables. Standardized data facilitates an unbiased comparison across variables and environments. Using MODIS standard products significant trends were observed in almost all variables between 2000-2017, including land surface temperature, percent snow covered area, NDVI, EVI, phenology, burned area, marine chlorophyll, CDOM, sea surface temperature, and marine primary productivity. Analysis of seasonal data revealed significant breakpoints in temporal trends. Within the terrestrial environment, data showed significant increasing trends in land surface temperature and NDVI. In the marine environment significant increasing trends were detected in primary productivity. Significantly earlier onset of green up date was observed in bioclimate subzones C&E and longer end of growing season in B&E. Terrestrial and marine parameters showed similar rates of change with unidirectional change in terrestrial and significant directional and magnitude shifts in marine.

[1] A version of this chapter is in press as Jenkins et al. 2019

Introduction

Climate change models consistently predict the greatest expected warming to occur in high northern latitudes. Similarly, reports from the Intergovernmental Panel on Climate Change (IPCC) convey the expectation that the Arctic region will warm 2-3 times more than the global mean (IPCC 2018). Models predict that the Arctic will warm 4.3-7.6°C by 2100 compared to the predicted global mean warming of 1.5-2.7°C (IPCC 2018). Proxy Arctic temperature records from the past 2000 years above 60°N latitude show the last half century being the warmest of the past two millennia, with the previous, long-term Arctic cooling trend being reversed during the 20th century (Kaufman et al. 2009).

A warmer Arctic is expected to have many physical and ecological consequences, all operating within a set of complex feedback mechanisms. Reduction in sea ice and permafrost, changes to surface hydrology, as well as shifts in vegetation zones, biomass, and productivity are among some of the expected primary consequences of a warmer Arctic. Secondary consequences include severe disruptions to biodiversity with anthropogenically-driven climate change being the most serious threat to biodiversity in the Arctic (Meltofte et al. 2013).

As the Arctic continues to experience a period of intense and accelerating change it has become increasingly important to expand access to information on the status and trends of Arctic biodiversity. The Arctic Council is the leading intergovernmental forum promoting cooperation, coordination, and interaction among the Arctic States, Arctic Indigenous Peoples

(represented by the Permanent Participants[2]) and other Arctic inhabitants on issues common within the Arctic, in particular, on issues of sustainable development and environmental protection in the Arctic. The Arctic Council has recommended that long-term monitoring efforts and inventories should be increased and focused to address key gaps in knowledge to better facilitate the development and implementation of conservation and management strategies (ACIA 2004; Meltofte et al. 2013) as well as take action on monitoring advice from what is presently known about Arctic ecosystems.

The Circumpolar Biodiversity Monitoring Program (CBMP) is the cornerstone program of the Conservation of Arctic Flora and Fauna (CAFF), the Arctic Council's biodiversity working group. The CBMP aims to be multi-knowledge based, utilizing science through bringing together an international network of scientists, government institutions, Indigenous organizations, and conservation groups working to harmonize and integrate efforts to monitor the Arctic's living resources. Its goal is to facilitate understanding, and more rapid detection and communication of significant biodiversity-related trends and pressures affecting the circumpolar world, while also establishing international linkages to global biodiversity initiatives.

Implementing the CBMP across marine, terrestrial, freshwater, and coastal ecosystems has largely focused on evaluation of *in situ* data collected across a myriad of focal ecosystem components (FECs). The CBMP has identified key elements, called FECs, of Arctic marine, freshwater, terrestrial and coastal ecosystems. Changes in FEC status likely indicate changes in

[2] The Arctic Council Permanent Participants are Aleut International Association; Arctic Athabaskan Council; Gwich'in International; Inuit Circumpolar Council; Saami Council; Russian Association of indigenous Peoples of the North

the overall environment and are therefore monitored. Field data collection in the Arctic is logistically and financially challenging and these data remain sparse and disparate, as described in the first of the CBMP State of the Arctic Terrestrial Biodiversity Report (CAFF 2017) and documented throughout this special issue. Recognizing the challenges associated with field data collection in the Arctic and the need for a more comprehensive understanding of change across the Arctic, CAFF initiated the Land Cover Change (LCC) Initiative to evaluate remote sensing for use in Arctic biodiversity monitoring and assessment activities. The work presented here is the result of the CAFF Land Cover Change Initiative.

Climate warming has not been uniform across the pan-Arctic region (Hansen et al. 1999) and responses to warming are expected to similarly exhibit spatial variability (Stow et al. 2004). Large scale synoptic monitoring tools are needed to assess baseline conditions and detect change and to conduct these analyses across a range of spatial and temporal scales. Remote sensing has the ability to provide these tools as data are available at a variety of spatial, temporal, and radiometric scales.

Several satellites have been designed specifically to provide datasets for ecosystem monitoring at a global scale. Historically the main systems used in studies across the pan-Arctic have included AVHRR (1978-present) and MODIS (1999-present). Studies using AVHRR have been limited by spatial resolution with one pixel covering approximately 1 km^2 of land. With the launch of two MODIS satellites in the early 2000s, data are available at a much higher spatial resolution (up to 250-meter), while also matching AVHRR's almost-daily global cover and exceeding its spectral resolution. MODIS provides images over a given pixel of land just as often as AVHRR, but in much finer detail and with measurements in a greater number of wavelengths

using detectors that were specifically designed for measurements of ecosystem dynamics. The European Space Agency's (ESA) Sentinel program, with the first satellite launched in 2014, continues the path of technological innovation in the field of remote sensing and provides robust earth observation data through a family of missions with each mission based on a constellation of two satellites.

Despite many technological advances in satellite systems, the Arctic presents many challenges to remote sensing based studies due to persistent cloud cover and haze, snow cover, limited solar illumination, and changing solar zenith angles. Remote sensing scientists have worked to overcome these challenges by identifying systematic bias and developing data processing algorithms to account for these effects. Most notably, cloud cover has been shown to bias land surface temperature (Westermann et al. 2011) and NDVI (Karami et al. 2017). Solutions typically employ mathematics to smooth and remove cloud-induced noise. Other solutions include fitting a model to the data that mimics expected behavior, such as using a sinusoidal model to reproduce seasonal variations (Hachem et al. 2009), or to gap fill cloud-contaminated satellite data using estimates from empirical relationships.

Remote sensing data have frequently been used for specific disciplinary studies at focused locations across the Arctic. Fewer large scale studies at the landscape or pan-Arctic scale have been conducted, but these studies do indicate strong signals of ecosystem change in the terrestrial environment, especially related to vegetation greening (Jia et al. 2003; Goetz et al. 2005; Bhatt et al. 2010, 2013; Reichle et al. 2018), an increase in shrub cover and decrease in freshwater surface area (Stow et al. 2004). Pan-Arctic studies of marine environments also indicate significant change, including a decline in Arctic sea ice extent (Stroeve and Meier 2018,

Parkinson et al. 1999; Comiso et al. 2008; Frey et al. 2015) and increasing trends in Arctic marine primary productivity (Arrigo et al. 2008; Hill et al. 2012).

Remote sensing determination of vegetation "greening" are often based on the normalized difference vegetation index (NDVI). The NDVI is a remote sensing-based quantification using visible and near-infrared light reflected by vegetation. Many studies of NDVI show a strong correlation to *in situ* percent vegetation cover measurements in the Arctic (Hope et al. 1993; Stow et al. 1993; Laidler et al. 2007). Using NDVI, recent research points to spatial heterogeneity with an ongoing general greening trend starting in the 1980s (Jia et al. 2003; Goetz et al. 2005; Bhatt et al. 2010, 2013; Reichle et al. 2018). NDVI has also been linked to measurements of the Arctic growing season (McDonald et al. 2004; Park et al. 2016). The NDVI has been the standard remote sensing-derived vegetation index for decades, being used in a wide variety of vegetation studies globally. With the launch of MODIS, the enhanced vegetation index (EVI) was developed to reduce background and atmospheric noise and to eliminate saturation in high-biomass regions (Huete et al. 1999). NDVI are EVI are computed similarly and exploit the same relationship between red and NIR wavelengths, with EVI additionally using data from the blue band and some aerosol resistance terms. In the presence of snow, NDVI decreases, while EVI increases (Huete et al. 2002), which is an important distinction to consider in remote sensing based studies across the pan-Arctic.

Previous work on detecting trends in Arctic vegetation phenology from remote sensing have indicated longer growing seasons, primarily due to an earlier start of growing season by 4.7 days per decade and a delayed end of growing season by 1.6 days per decade over the observation period of 2000-2010 in high northern latitudes (Zeng et al. 2011). Estimates in

phenology shifts were shown to differ in North America and Eurasia with North America having a significantly earlier start of season and a slightly later end of season (Zeng et al. 2011). North America also appears to be "greening" to a greater extent than Eurasia (Dye and Tucker 2003, Bunn et al. 2007, Bhatt et al. 2010).

Five Arctic tundra bioclimatic zones have been identified and mapped in the Circumpolar Arctic Vegetation Map (CAVM Team 2003). These delineations are described as subzones A-E ranging from North to South with Subzone A being the coldest and Subzone E the warmest. These bioclimatic zones have been used to describe Arctic vegetation trends in many scientific studies (Epstein et al. 2012, Jia et al. 2009, Reichle et al. 2018) and represent an ecologically meaningful way to divide the Arctic for trend reporting.

In addition to studies on vegetation, satellite remote sensing data has shown a decline in freshwater surface area attributed to degradation of permafrost in the Arctic since the 1950s (Smith et al. 2005; Riordan et al. 2006; Carroll et al. 2011). In Siberia, there is a decreasing trend in Arctic lake abundance since the early 1970s (Smith et al. 2005). In Arctic Alaska, remote sensing data validated with field surveys have also shown a decrease in a majority of pond surface area from 1950 to 2000 (Stow et al. 2004). From 2003 to 2010, satellite microwave remote sensing data also shows seasonal and annual variability in surface inundation in Arctic Alaska with wetting trends within continuous and discontinuous permafrost zones and drying trends in sporadic and isolated permafrost zones (Watts et al. 2012).

The objective of this paper is to demonstrate the applicability of remote sensing as a multi-parameter monitoring tool for implementation within the CBMP. Data from this study will begin a formation of baselines and provide a pan-Arctic understanding of the status of spatial

and temporal trends across multiple parameters simultaneously. The goal is to measure magnitudes and rates of change and to develop a methodology for synoptic monitoring in the pan-Arctic going forward.

Materials and Methods

Remote sensing data used in this study are from the MODIS (Moderate Resolution Imaging Spectroradiometer) instrument aboard the Terra and Aqua satellites. MODIS data are acquired every 1 to 2 days worldwide in 36 spectral bands, with more frequent coverage in the Arctic due to the sun-synchronous satellite orbit providing up to 4 daily overpasses. Aside from raw radiometric data, MODIS data are available in a variety of derived products that span many disciplines and applications. MODIS standard data products are used in this study to provide a common data input across all investigated parameters. The specific remote sensing products used in this study are detailed with metadata in Table 1. Time periods of observation range from 14 to 18 years. MODIS standard data products are used for all study parameters with the exception of sea ice extent. For this parameter, a combined passive microwave satellite product (Stroeve and Meier 2017) from SMMR and SSM/I-SSMIS are used.

Table 2-1. *A set of remote sensing-based physical and ecological parameters in both the marine and terrestrial pan-Arctic environments were analyzed in this study. This table outlines the parameters and metadata, including the spatial and temporal selection.*

Physical and Ecological Parameters	Satellite Platform, Product Name and Version Number	Temporal Selection Available	Temporal Selection Used	Spatial Resolution	Data Source
Land Surface Temperature (LST), Day	MODIS Terra; MOD11C3; 6	Monthly, 2000-2017	2001-2017, Jan-Dec	0.05deg (~5,600m)	LPDAAC
Percent Snow Covered Area (Snow)	MODIS Terra; MOD10CM; 6	Monthly, 2000-2017	2003-2017, Mar-Oct	0.05deg (~5,600m)	NSIDC
Normalized Difference Vegetation Index (NDVI)	MODIS Terra; MOD13C1; 6	16-day; 2000-2017	2001-2017, May-Sep	0.05deg (~5,600m)	LPDAAC
Enhanced Vegetation Index (EVI)	MODIS Terra; MOD13C1; 6	16-day; 2000-2017	2001-2017, May-Sep	0.05deg (~5,600m)	LPDAAC
Green Up Date	MODIS Aqua, Terra; MCD12Q2; 5	Yearly, 2001-2014	2001-2014	500m	LPDAAC
Senescence Date	MODIS Aqua, Terra; MCD12Q2; 5	Yearly, 2001-2014	2001-2014	500m	LPDAAC
Growing Season Length (GSL)	MODIS Aqua, Terra; MCD12Q2; 5	Yearly, 2001-2014	2001-2014	500m	LPDAAC
Burned Area	MODIS Aqua, Terra; ABBA; 2	Yearly, 2001-2015	2001-2015	500m	Loboda et al. 2017
Marine Chlorophyll (Chl)	MODIS Aqua; MO_chlor_a; 2014.0	Monthly, 2003-2017	2003-2017, Apr-Oct	4km	NASA OceanColor
Colored Dissolved Organic Material (CDOM)	MODIS Aqua; MO_IOP_adg_443_giop; NA	Monthly, 2003-2017	2003-2017, Apr-Oct	4km	NASA OceanColor
Sea Surface Temperature (SST)	MODIS Aqua; MO_SST4; 2014.0	Monthly, 2003-2017	2003-2017, Jan-Dec	4km	NASA OceanColor
Marine Primary Productivity (PP)	MODIS Aqua; VGPM; NA	Monthly, 2003-2016	2003-2016, Apr-Oct	9km	O'Malley 2017
Sea Ice Extent	Combined Passive Microwave (SMMR and SSM/I-SSMIS); 2	Monthly, 1978-2016	2003-2016, Jan-Dec	25km	NSIDC

Systematic biases and known areas of concern for each MODIS data product are documented in the Algorithm Theoretical Basis Documents (ATBS's) and throughout the scientific literature. Data quality flags are developed based upon these concerns, but treatment varies significantly product-to-product. Some products have quality flags with limited usefulness. For example, the snow covered area product used in this analysis (MOD10CM) only reports pixels as having "good" or "other" quality. In order to get more detailed quality information, one must look at the quality flags in the lower level data that feeds into the monthly-aggregated product used in this analysis (Riggs and Hall, 2016). There are other known

limitations of the products used here. These issues include difficulty distinguishing snow and clouds in the snow cover product (Hall and Riggs, 2007); lower quality phenology detections due to high solar zenith angles, snow, and cloud cover; and land surface temperature biases due to cloud cover contamination (Westermann et al. 2011). Data quality flags, when available, have been applied to the data in this study to limit effects from cloud cover and snow, but no additional smoothing or model fitting were conducted.

The remote sensing data products were converted from their source format to a GeoTIFF, re-projected into the Lambert Azimuthal Equal Area projection, and clipped to the CAFF pan-Arctic extent. The terrestrial and combined MODIS products from LPDAAC were processed using the HDF-EOS to GeoTIFF Conversion Tool (HEG Tool; HEG 2017), and the Aqua MODIS products and non-MODIS products were processed using the Geospatial Data Abstraction Library (GDAL; GDAL 2017). MODIS MCD12Q2 products were distributed as tiles and were stitched together using ESRI's Mosaic to New Raster tool after re-projection.

The data used in this analysis, including the fully-processed and clipped versions, have been archived at the Arctic Biodiversity Data Service (ABDS, https://www.abds.is/) under Land Cover Change. Additional geospatial data layers used in this analysis reside at this location as well as pan-Arctic headline indicator data, CBMP data, boundaries, and sensitive and protected areas data.

Remote sensing data were used to calculate average annual and seasonal time series over the 14 to 18 year observation periods. These analyses were performed at the pan-Arctic level as well as within defined analysis areas. In addition to the pan-Arctic extent, marine parameters were analyzed by high, low, and sub Arctic areas and terrestrial parameters were

analyzed by the five bioclimate subzones defined by the Circumpolar Arctic Vegetation Map, CAVM (CAVM Team 2003). Figure 1 shows the geospatial boundaries of the analysis areas.

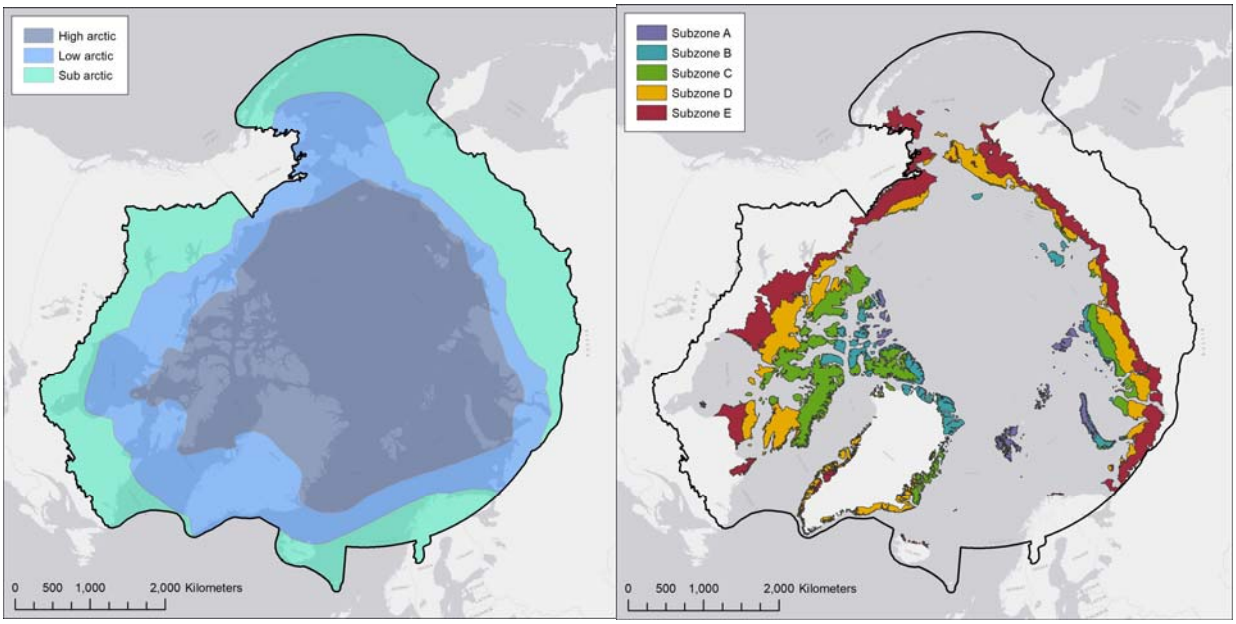

Figure 2-1. *In addition to the entire pan-Arctic extent, several geographic analysis areas were used to parse data and report findings, including high, low, and sub Arctic (left) and the CAVM bioclimate zones (right).*

Data were standardized to facilitate a uniform comparison between parameters and between the terrestrial and marine environments. For each variable, each data point was standardized by subtracting the variable's mean over its entire temporal span and dividing by the variable's standard deviation over the same temporal span. After standardization, all parameter datasets are unitless with a mean of zero and standard deviation of 1.

All statistical analyses were conducted in R (R Core Team 2015). After aggregating data to the yearly level, annual trends were analyzed using ordinary least squares (OLS) regression and slope significance was determined using a two tailed t-test with a p-value threshold of 0.05.

The BFAST package in R (Breaks for Additive Seasonal and Trend; Verbesselt et al. 2010) was also used to identify long-term trends in the parameters and to identify breakpoints, if present, in the time series where monthly or 16-day seasonal data was available. This approach decomposes a time series into trend, seasonal, and remainder components and searches for significant changes or breakpoints in the trend or seasonal components. A minimum segment size of 3 years (representing approximately 20% of the data record as was used in Verbesselt et al. 2010) was set to avoid the detection of short-term anomalies. When significant breakpoints were identified, the slope and its significance were reported for each side of the change.

Results

This study identified statistically significant temporal rates of change in many physical and ecological parameters, whether assessed across the pan-Arctic as a whole or analyzed by regions or subzones. Different rates of change as well as magnitude and directional shifts in trends were also detected. In terms of annual versus seasonal data more statistically significant trends were identified in the seasonal data in both the terrestrial and marine parameters.

The power of parsing data by geospatial regions is shown in the average annual land surface temperature plots in Figure 2. A clear separation of the data by bioclimate subzone is observed in Figure 2A, which generally follows latitudinal trends. While subzones A, B, D and E all experienced significant increases in temperature across the observation period, the highest temperatures were seen in the southernmost zones (D and E). Standardizing the data more clearly shows how the rate of change of temperature varies across the regions (Figure 2B). Subzone A exhibited the greatest increase (slope=0.146), followed by subzones E, B, and D (slopes = 0.124, 0.11, and 0.103, respectively).

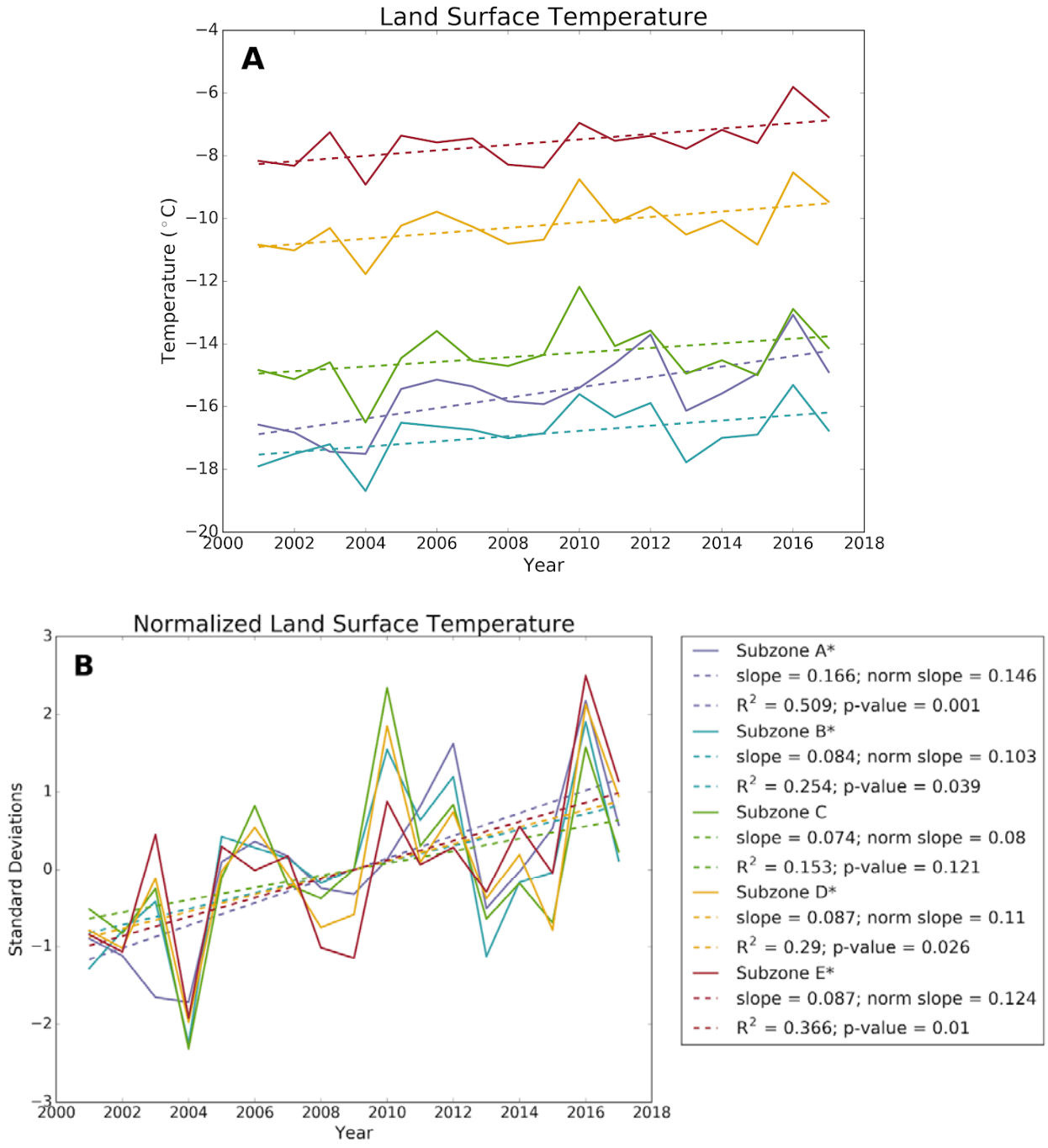

Figure 2-2. *Plots of land surface temperature by bioclimate CAVM subzones show a clear separation of temperature within the different zones. Panel A shows the non-standardized data. Subzones A, B, D, & E have statistically significant increasing trends as indicated by an asterisk in the legend (p-values 0.001, 0.039, 0.026, & 0.010, respectively). Disregarding the absolute differences, the standardized plot (panel B) more clearly shows the common shifts in rates and directions of change as well as differences among subzones. CAVM subzone A, the northernmost zone, showed the greatest rate of overall increase in land surface temperature, followed by subzones E, B, and D.*

Monthly land surface temperature data also showed heterogeneous responses between CAVM subzones. For instance, subzone A exhibited significant increasing trends in January, February, March, April, September, October, and November (p-values = 0.031, 0.028, 0.002, 0.04, 0.026, 0.002, and 0.012, respectively). Subzone E, the southernmost vegetation zone, also showed increasing trends, but only in the months April, May, and June (p-values = 0.016, 0.01, and 0.004, respectively). This indicates that while nearly all CAVM subzones exhibited significant rises in average land surface temperature over the 2001-2017 observation period, there was north-south variability in the seasonality of temperature change. The northernmost CAVM subzone experienced significant rising temperature trends in fall, winter, and spring, while the southernmost CAVM subzone showed a significant rising temperature trend in late spring to early summer.

The aggregated average annual pan-Arctic data showed statistically significant temporal trends in land surface temperature and NDVI ($p=0.04$ and $p<0.001$, respectively; Fig. 3). The standardized rate of change in NDVI was greater than that of temperature (0.166 and 0.099, respectively). EVI was also assessed with similar results to NDVI in all analysis areas. The average annual data indicated that both land surface temperature and NDVI were significantly increasing in CAVM subzones A, B, D, and E (p-values in Table 2). The BFAST analysis, by incorporating seasonal variability, showed similar results for the pan-Arctic and these subzones while also indicating a significantly increasing trend both parameters in CAVM subzone C. This analysis also indicated a breakpoint in 2013 for CAVM subzones B and C such that the land surface temperature rate of increase became significantly higher.

In terms of terrestrial phenology, three different parameters were analyzed: greenup date, senescence date, and growing season length. No significant trends were observed in senescence date. Subzones C and E showed a statically significant decrease for the green up date, indicating that the growing season shifted to an earlier start date over time (changes of 4.5 and 4 days over 14 years, respectively). Related to this, subzones B and E showed a statistically significant increase in growing season length (with changes of 5 and 3.5 days, respectively). BFAST analysis was not applied to phenology data since there is only one value for each parameter each year (i.e., there is no monthly green up date).

No significant trends were observed in the average annual percent snow covered areas, though looking at time series for individual months did reveal significant trends. Significant declining trends were observed in Subzones C and D for the month of June (p-value=0.020 and 0.028), Subzone E for the month of July (p-value=0.013), and Subzones A and B for the month of October (p-value=0.005 and 0.033). Observations of the seasonal data within the changepoint analysis revealed significant declining trend from 2000-2011 (p-value=0.019) followed by a significant increasing trend from 2011-2014 in Subzone B (p-value<0.001). No other significant seasonal trends were identified.

No trends were found in the measures of amount of average annual burned area across the pan-Arctic. Burned area polygons were not present in subzones A and B. The burned area product is only available at a yearly time scale so the seasonal breakpoint analysis could not be performed.

By standardizing the data we can see that the terrestrial and marine environments have both experienced somewhat similar amounts of change, when expressed as standardized

standard deviation from each variable's mean (Figure 3). The change plots show the standardized parameters and their positive or negative rate of change. In the marine environment two parameters, sea ice and primary productivity, showed significant change over the observation period. In the terrestrial environment, parameters are more closely grouped with NDVI and land surface temperature showing the greatest rate of change. Interestingly, the rates of change of NDVI and sea ice were approximately the same (0.166 & -0.168, respectively). The detailed statistics for the rates of change and significance values are shown in Table 2.

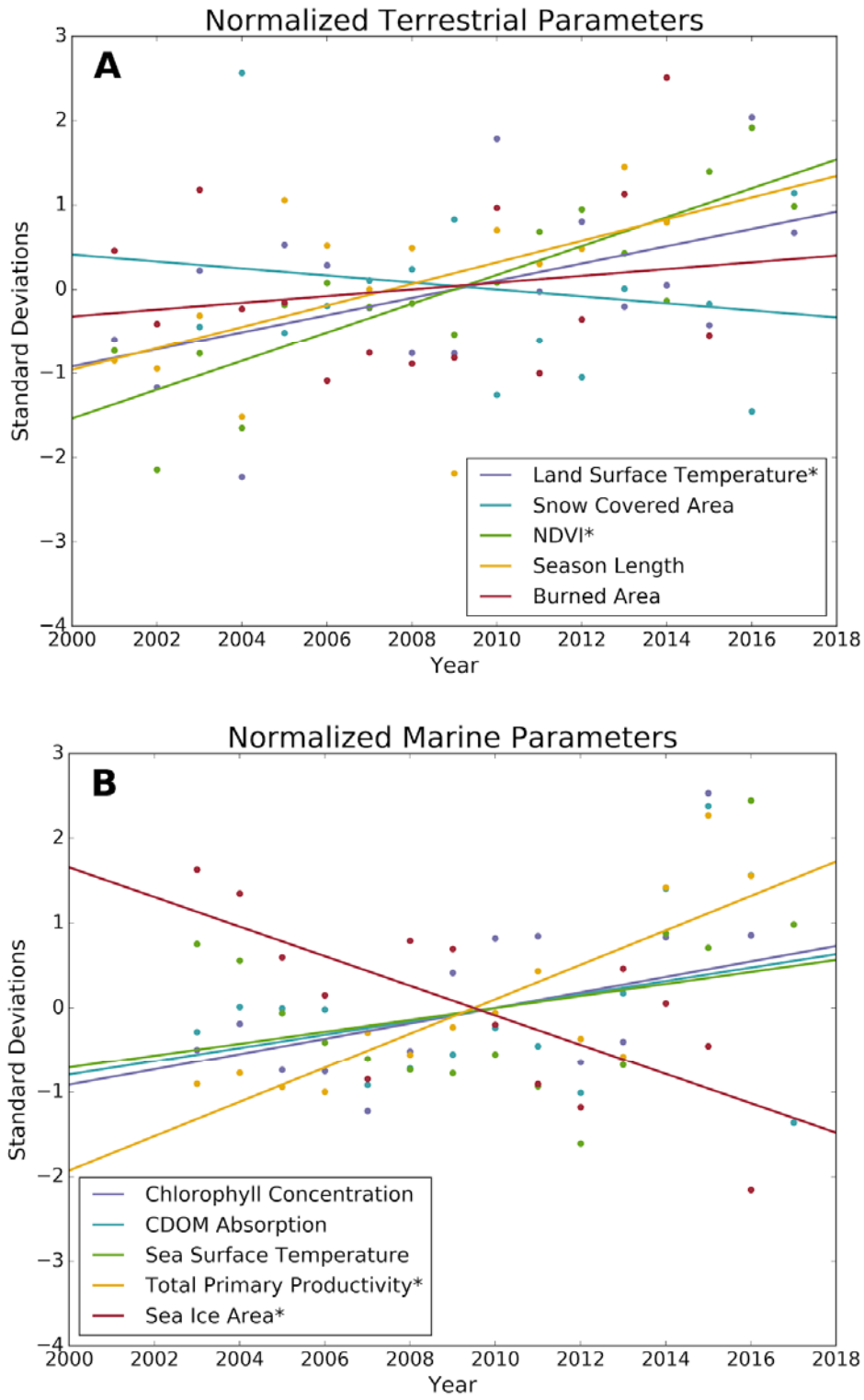

Figure 2-3. *Average annual standardized data across the pan-Arctic showing rates of change among the different parameters and compare the terrestrial (panel A) with the marine (panel B) environments. Statistically significant trends ($p < 0.05$, test of slope different from zero) are marked with an * in the legend. Detailed statistics for the trends are available in Table 2.*

Table 2-2. *Summary rates of change for the standardized data and the associated p-values in parentheses. Statistically significant temporal trends (p < 0.05) are bolded and marked with an asterisk (*).*

Terrestrial	**Land Surface Temp**	**Snow Cover**	**NDVI**	**Green Up**	**Senescence**	**Season Length**	**Burned Area**
Pan-Arctic	**0.099 (0.041*)**	-0.040 (0.524)	**0.166 (<0.001*)**	-0.125 (0.056)	-0.062 (0.368)	0.123 (0.059)	0.039 (0.537)
Subzone A	**0.141 (0.001*)**	0.011 (0.862)	**0.155 (<0.001*)**	-0.004 (0.956)	0.0409 (0.559)	0.079 (0.247)	NA
Subzone B	**0.100 (0.039*)**	-0.020 (0.749)	**0.148 (0.001*)**	-0.099 (0.142)	-0.009 (0.897)	**0.1336 (0.038*)**	NA
Subzone C	0.077 (0.121)	-0.060 (0.335)	0.080 (0.107)	**-0.135 (0.036*)**	-0.125 (0.054)	0.066 (0.340)	NA
Subzone D	**0.107 (0.026*)**	-0.081 (0.184)	**0.143 (0.001*)**	-0.097 (0.148)	-0.063 (0.364)	0.104 (0.119)	0.002 (0.971)
Subzone E	**0.120 (0.010*)**	-0.045 (0.475)	**0.156 (<0.001*)**	**-0.129 (0.047*)**	-0.028 (0.688)	**0.147 (0.019*)**	-0.060 (0.335)
Marine	**Chlorophyll**	**CDOM**	**Sea Surface Temp**	**Sea Ice (2003-2017)**	**Total PP**		
Pan-Arctic	0.088 (0.146)	0.076 (0.212)	0.068 (0.268)	**-0.168 (0.005*)**	**0.196 (<0.001*)**		
High Arctic	0.094 (0.117)	0.078 (0.200)	0.103 (0.085)	**-0.172 (0.004*)**	**0.174 (0.003*)**		
Low Arctic	0.093 (0.124)	0.0728 (0.236)	0.087 (0.152)	-0.026 (0.710)	**0.152 (0.015*)**		
Sub Arctic	0.044 (0.479)	0.078 (0.206)	0.075 (0.220)	0.080 (0.241)	0.093 (0.169)		

Observations of the seasonal data reveal changes in the seasonal dynamics. Figure 4 show the seasonal curves of the land surface temperature data over the two decadal time series. The BFAST statistical software identifies the line of best fit, incrementally, over the time series which may result in one or more lines of fit. Figure 4 shows changepoints in the land surface temperature data record for Subzones B and C. Both of these changepoint years occur in 2013 and indicate a magnitude shift from the 2001-2013 data record to the 2013-2017 record. That is to say, the warming trend accelerated during these time periods.

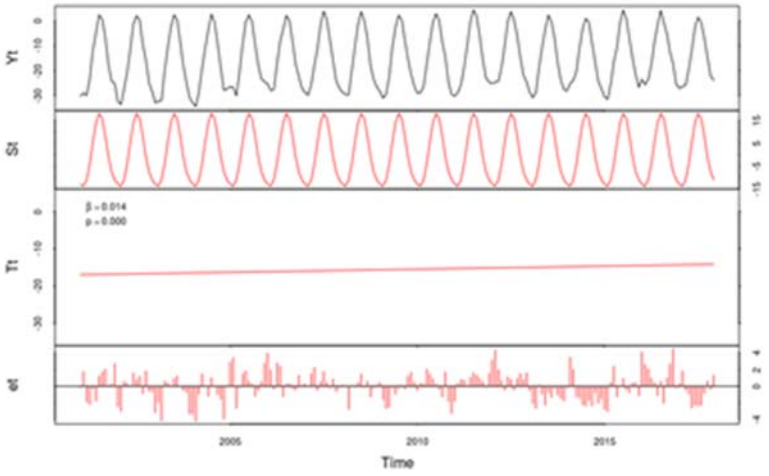

Subzone A

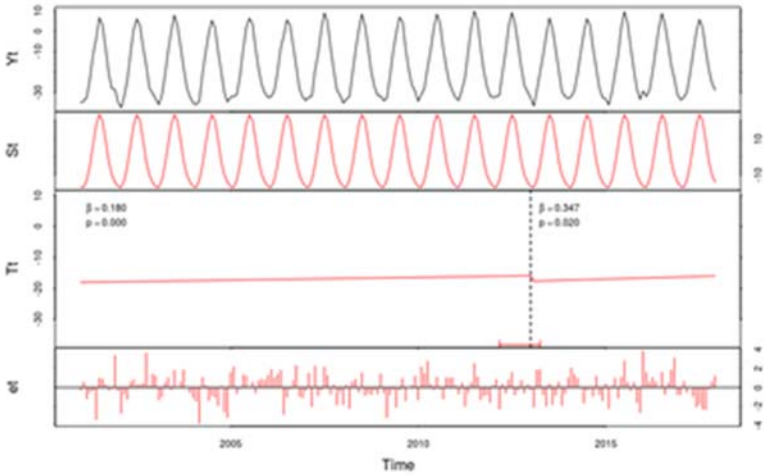

Subzone B

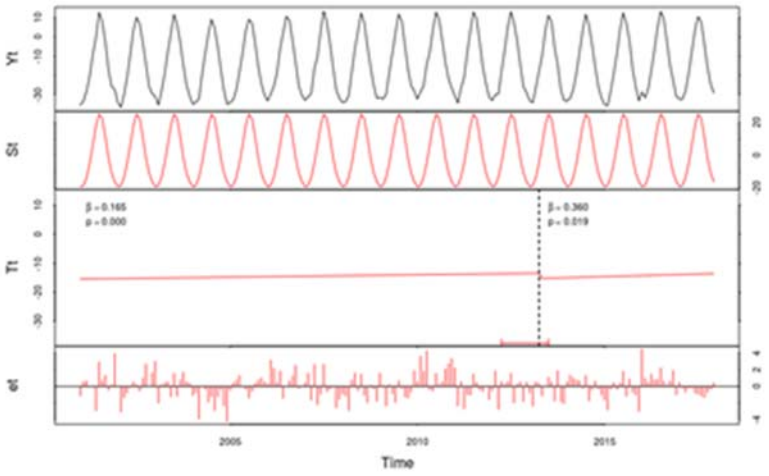

Subzone C

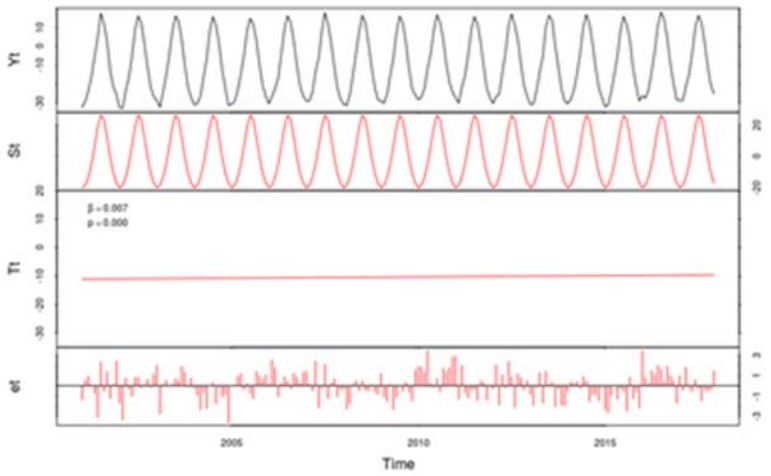

Subzone D

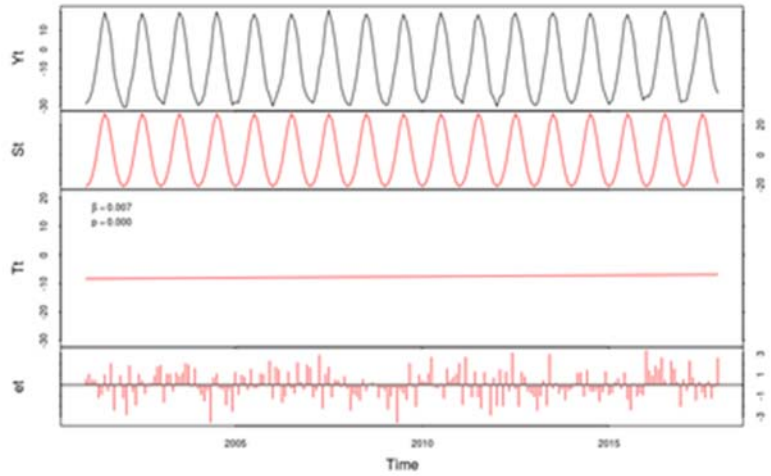

Subzone E

Figure 2-4. *Results from the BFAST changepoint analysis on the seasonal land surface temperature data show breaks in the trends in subzones B and C occurring in 2013 for both subzones. The trend for all subzones are statistically significant ($p < 0.05$) as indicated by the respective p-values printed in panel three of each subzone output. The output graphs show the fully plotted data in the top panel, followed by the seasonal trends. The third panel in each subzone output show the annual trend and any identified breaks in trend with associated error bars. The fourth panel shows the residual differences from the trend.*

Table 2-3. *Summary table showing the BFAST-derived trends and changepoints for parameters with seasonal data. Purple color indicates a statistically significant ($p < 0.05$) increasing trend, blue indicates a decreasing trend, and empty cells indicate no temporal change or a non-significant trend. Black cells indicate that a significant shift in a temporaltrend occurred in that year.*

Marine		2001	2002	2003	2004	2005	2006	2007	2008	2009	2010	2011	2012	2013	2014	2015	2016	2017
Chlorophyll	Pan-Arctic	na	na															
Chlorophyll	High Arctic	na	na															
Chlorophyll	Low Arctic	na	na															
Chlorophyll	Sub Arctic	na	na															
CDOM	Pan-Arctic	na	na															
CDOM	High Arctic	na	na															
CDOM	Low Arctic	na	na															
CDOM	Sub Arctic	na	na															
Sea Surface Temperature	Pan-Arctic	na	na															
Sea Surface Temperature	High Arctic	na	na															
Sea Surface Temperature	Low Arctic	na	na															
Sea Surface Temperature	Sub Arctic	na	na															
Sea Ice Area	Pan-Arctic	na	na															na
Sea Ice Area	High Arctic	na	na															na
Sea Ice Area	Low Arctic	na	na															na
Sea Ice Area	Sub Arctic	na	na															na
Total Primary Productivity	Pan-Arctic	na	na															na
Total Primary Productivity	High Arctic	na	na															na
Total Primary Productivity	Low Arctic	na	na															na
Total Primary Productivity	Sub Arctic	na	na															na
Terrestrial																		
Land Surface Temperature	Pan-Arctic																	
Land Surface Temperature	Subzone A																	
Land Surface Temperature	Subzone B																	
Land Surface Temperature	Subzone C																	
Land Surface Temperature	Subzone D																	
Land Surface Temperature	Subzone E																	
Percent Snow Cover	Pan-Arctic	na	na															
Percent Snow Cover	Subzone A	na	na															
Percent Snow Cover	Subzone B	na	na															
Percent Snow Cover	Subzone C	na	na															
Percent Snow Cover	Subzone D	na	na															
Percent Snow Cover	Subzone E	na	na															
NDVI	Pan-Arctic																	
NDVI	Subzone A																	
NDVI	Subzone B																	
NDVI	Subzone C																	
NDVI	Subzone D																	
NDVI	Subzone E																	

Discussion

A large number of parameters show a statistically significant temporal trend over the almost two-decade time series. This is of note in and of itself, but many of these statistically significant trends are also showing a magnitude or directional breakpoint within this limited temporal observation window.

Comparing many parameters simultaneously within the same methodological framework provides context and a frame of reference for observed change. For example, sea ice decline is frequently reported on in both the scientific and popular media, and the rate of change in sea ice extent is generally considered significant and alarming. Results from this study show that the rate of change in sea ice extent is comparable to total primary productivity, albeit in opposite directions. In the terrestrial environment, NDVI has similar rates of change to sea ice and primary productivity.

Study findings are temporally limited by the MODIS dataset in terms of number of years of observations. Many trends were marginally significant or have specific outlier years that affect the overall statistical significance. This is an indication that more changes may be occurring across the pan-Arctic than are being reported in this study and that more change may be on the horizon. Specifically, several of the marine parameters including primary productivity and sea surface temperature show an uptick in measurements during the final two observations years (2016 and 2017). Given a few more years of data, this could be determined to represent a shift to a new normal or an anomaly in the data record. Regardless, more data are needed in order to develop a better sense of the temporal variability of these parameters.

NDVI and EVI results are in agreement with other studies pointing to a “greening” trend across the pan-Arctic (Jia et al., 2003; Goetz et al., 2005; Bhatt et al., 2010, 2013; Reichle et al. 2018). Most studies use the NASA GIMMS dataset based on AVHRR satellite data for NDVI comparison. This effort focuses on MODIS satellite data and data products, providing yet another data record for corroboration of “greening” in the Arctic.

The vegetation phenology results show that the greenup date is moving earlier by nearly six days and the growing season length is extending by approximately 4 days over the 2001-2014 observation period across the pan-Arctic. This is consistent to what others have reported in the Arctic with Zeng et al. 2011 reporting a earlier start of season by 4.7 days and a later end of season by 1.6 days for the period 2000-2010, for areas N of 60° latitude, using MODIS NDVI data. These results are similar despite methodological differences in vegetation index computation, years of observations, and geographic region of analysis. The MODIS vegetation phenology product (MCD12Q2) used in this study is based on EVI data where many other studies of phenological trends use NDVI data (Zeng et al. 2013, Zeng et al. 2011, Karami et al. 2017). In this study we also found a greater year-to-year variability in the date of senescence than greenup, with results showing a somewhat cyclical trend.

In the marine environment, 2013/2014 appears to be a tipping point in which the directionality and/or trend significance of several different parameters changed. Table 3 shows the specific breakpoints and includes significant breaks for all marine parameters and across all Arctic zones. Of note are that the pan-Arctic sea surface temperature shifted from a significant decreasing trend to a significant increasing trend in 2013 and CDOM showed a shift from an increasing trend to a decreasing trend in 2014 in all zones.

The marine parameters are more variable than the terrestrial parameters in terms of magnitude and directional shifts and the number of breakpoints. The trends in the terrestrial parameters are essentially all unidirectional. Going forward, the feedback mechanisms and the relationships between the marine and terrestrial parameters need to be investigated.

It is important to recognize the potential issues associated with the remote sensing data products used in this analysis. In this study we applied the MODIS quality flags, when available, to reduce effect from clouds and snow but data artifacts still remain. We generally included more pixels than other discipline-specific studies or studies from specific geographic locations due to unknown and variable weather and climate scenarios and data artifacts across all the parameters and across the entire pan-Arctic. Additional noise filtering in our dataset has been provided by averaging the data over large geographic regions. Data standardization also serves to further smooth noise. There are many excellent solutions in the literature to achieve a more accurate satellite data record by combining satellite inputs with ground observations, models, and mathematics, and these solutions should be employed when working with absolute data and trend analysis for specific parameters.

A goal of the MODIS data products is to continually improve the retrieval algorithms and to provide these updates to the user community through version updates. Over time these remote sensing products will improve in accuracy and precision with better documentation of known issues. Additionally, the scientific community will continue to evaluate these products through comparisons to ground observations and models.

The relatively short MODIS data record (14-17 points depending on parameter) also limits our ability to make decisive conclusions about trends in the annual mean. Because the OLS regression approach is sensitive to extreme values, even a single outlier in the dataset could result in the conclusion of a significant trend. Additionally, the OLS assumption of homogeneity can fail if there is a discontinuity or breakpoint in the data (Lanzante, 1996) or as a result of seasonal variation (de Jong and de Bruin, 2012). Aggregating the data to a yearly level can also potentially mask interesting shifts in seasonal variability. For instance, an increase in annual mean surface temperature could be due to increased temperatures across the entire year, or it could be that the summers are getting warmer while the winter temperatures remain steady. The BFAST approach, which extracts long-term and seasonal trends from the full, non-aggregated dataset, is able to account for seasonal variability in identifying trends while also identifying significant breakpoints in both long-term and seasonal trends (Verbesselt et al., 2010). BFAST has been used in numerous remote sensing time series analyses (de Jong et al., 2012; Lambert et al., 2013), and is likely a more effective tool for future investigation of Arctic trends and shifts. It is important to note however, that the minimum segment size allowed between changepoints (a parameter within the BFAST tool) could result in biases due to climatological phenomena such as the North Atlantic oscillation (NAO), Arctic oscillation (AO) and the Atlantic multidecadal oscillation (AMO).

As stated, one of the objectives of this paper is to demonstrate the applicability of remote sensing as a multi-parameter monitoring tool (meaningful to implementation of the CBMP). The use of MODIS based remote sensing as an observation tool is self-evident, although work remains to better understand uncertainty in the presented (and other) remote

sensing derived focal ecosystem states and changes. That is, how is measurement uncertainty impacting results and therefore how reliably can remote sensing tools, exceptional for observation, be used for monitoring? Individual results presented here and discussed above do provide a synoptic view of change in the Arctic and change by biologically meaningful reporting units (marine and CAVM bioclimate subzones), and corroborate past finding of change in the Arctic; but, the real power here is two-fold, understanding of the status of spatial and temporal trends across multiple parameters simultaneously, and serving as potential explanatory variables for *in situ* changes observed across the myriad CBMP focal ecosystem components.

Conclusions

MODIS is a powerful monitoring and analysis tool for the Arctic in terms of spatial coverage of the entire pan-Arctic on a daily timescale. The growing season in the Arctic is short and the temporal resolution afforded by MODIS is needed in order to capture phenological and seasonal changes occurring on a daily to weekly scale. Having daily data also provides the ability to account for cloud cover in the Arctic through composite images. The sea ice data provided by passive microwave in this study complements the electro-optical MODIS data products. Passive microwave data, which are not affected by cloud cover or solar illumination, provide valuable data during the winter months.

The analyses presented here should be updated every few years to provide a data stream useful for monitoring programs such as CBMP. This study, and many others, show significant change is occurring in the Arctic. We need to determine how resilient the Arctic is to these changes and where there may be certain thresholds, known also as “tipping points”, beyond which an abrupt shift of physical or ecological states occur. The changepoint analysis

presented here is a departure point for more detailed studies at different scales. *In situ* data from monitoring stations across the pan-Arctic may provide valuable calibration and validation data as well as provide early warning data to guide remote-sensing based parameter selection and algorithm development. Only with a combination of *in situ* data, remote sensing data, and an understanding of the processes occurring at different scales can we begin to understand change in the Arctic.

References

ACIA (2004) Impacts of a warming arctic: Arctic climate impact assessment. ACIA Overview Report. Cambridge University Press.

Arrigo, K.R., G. van Dijken, S. Pabi (2008) Impact of shrinking Arctic ice cover on marine primary productivity. Geophysical Research Letters, 35(19): L19603. https://doi.org/10.1029/2008GL035028

Bhatt, U.S., Walker, D.A., Raynolds, M.K., Comiso, J.C., Epstein, H.E., Jia, G., Gens, R., Pinzon, J.E., Tucker, C.J., Tweedie, C.E., Webber, P.J. (2010) Circumpolar arctic tundra vegetation change is linked to sea ice decline. Earth Interactions, 14: 1-20. https://doi.org/10.1175/2010EI315.1

Bhatt, U., Walker, D., Raynolds, M., Bieniek, P., Epstein, H., Comiso, J., Pinzon, J., Tucker, C., Polyakov, I. (2013) Recent declines in warming and vegetation greening trends over pan-arctic tundra. Remote Sensing, 5(9): 4229-4254. https://doi.org/10.3390/rs5094229

Bunn, A.G., Goetz, S.J., Kimball, J.S., Zhang, K. (2007) Northern high-latitude ecosystems respond to climate change. Eos, Transactions American Geophysical Union, 88(34), pp.333-335.

CAFF (2017) State of the Arctic Marine Biodiversity Report. Conservation of Arctic Flora and Fauna International Secretariat, Akureyri, Iceland. 978-9935-431-63-9

Carroll, M.L., J.R.G. Townshend, C.M. DiMiceli, T. Loboda, R.A. Sohlberg (2011) Shrinking lakes of the Arctic: Spatial relationships and trajectory of change. Geophysical Research Letters, 38: L20406. https://doi.org/10.1029/2011GL049427

CAVM Team (2003) Circumpolar Arctic vegetation map. Scale 1 : 7 500 000. Conservation of Arctic Flora and Fauna (CAFF) Map No. 1. US Fish and Wildlife Service, Anchorage, Alaska, USA, retrieved 1 December, 2016, from http://www.geobotany.uaf.ed383-50-1292u/cavm/.

Comiso, J.C., C.L. Parkinson, R. Gersten, L. Stock (2008) Accelerated decline in the arctic sea ice cover. Geophysical Research Letters, 35(1): L01703. https://doi.org/10.1029/2007GL031972

de Jong, R., J. Verbesselt, M.E. Schaepman, S. de Bruin (2012) Trend changes in global greening and browning: contribution of short-term trends to longer-term change. Global Change Biology, 18(2), 642-655. https://doi.org/10.1111/j.1365-2486.2011.02578.x

de Jong, R., S. de Bruin (2012) Linear trends in seasonal vegetation time series and the modifiable temporal unit problem. Biogeosciences, 9(1), 71-77. https://doi.org/10.5194/bg-9-71-2012

Dye, D.G., C.J. Tucker (2003) Seasonality and trends of snow-cover, vegetation index, and temperature in northern Eurasia. Geophysical Research Letters, 30(7). https://doi.org/10.1029/2002GL016384

Epstein, H.E., M.K. Raynolds, D.A. Walker, U.S. Bhatt, C.J. Tucker, J.E. Pinzon (2012) Dynamics of aboveground phytomass of the circumpolar Arctic tundra during the past three decades. Environmental Research Letters, 7(1), 015506. https://doi.org/10.1088/1748-9326/7/1/015506

Frey, K.E., G.W.K. Moore, L.W. Cooper, J.M. Grebmeier (2015) Divergent patterns of recent sea ice cover across the Bering, Chukchi, and Beaufort seas of the pacific arctic region. Oceanography, 136(2015): 32-49. https://doi.org/10.1016/j.pocean.2015.05.009

GDAL (2017) GDAL - Geospatial Data Abstraction Library: Version 2.2.3, Open Source Geospatial Foundation, retrieved 1 December, 2016, from http://gdal.osgeo.org

Goetz, S.J., A.G. Bunn, G.J. Fiske, R.A. Houghton (2005) Satellite-observed photosynthetic trends across boreal North America associated with climate and fire disturbances. Proceedings of the National Academy of Sciences, 102(38): 13521-13525. https://doi.org/10.1073/pnas.0506179102

Hachem, S., M. Allard, C. Duguay (2009) Using the MODIS land surface temperature product for mapping permafrost: an application to Northern Quebec and Labrador, Canada. Permafrost and Periglacial Processes, 20(4), 407-416. https://doi.org/10.1002/ppp.672

Hall, D.K., G.A. Riggs (2007) Accuracy assessment of the MODIS snow products. Hydrological Processes: An International Journal, 21(12), 1534-1547. https://doi.org/10.1002/hyp.6715

Hansen, J., R. Ruedy, J. Glascoe, M. Sato (1999) GISS analysis of surface temperature change. Journal of Geophysical Research, 104: 30997-31022. https://doi.org/10.1029/1999JD900835

HEG. 2017. HDF-EOS to GeoTIFF Conversion Tool (HEG), Version 2.14, Earth Observing System (EOS) Program, National Aeronautics and Space Administration, retrieved 1 December, 2016, from https://newsroom.gsfc.nasa.gov/sdptoolkit/HEG/HEGHome.html

Hill, V.J., P.A. Matrai, E. Olson, S. Suttles, M. Steele, L.A. Codispoti, R.C. Zimmerman (2012) Synthesis of integrated primary production in the Arctic Ocean: II. In situ and remotely sensed estimates. Oceanography, 110(2013): 107-125. http://dx.doi.org/10.1016/j.pocean.2012.11.005

Hope, A.S., J.S. Kimball, D.A. Stow (1993) The relationship between tussock tundra spectral reflectance properties and biomass and vegetation composition. International Journal of Remote Sensing, 14(10): 1861-1874. https://doi.org/10.1080/01431169308954008

Huete, A., C. Justice, W. van Leeuwen, W (1999) MODIS vegetation index (MOD13). Algorithm theoretical basis document, 3, 213.

Huete, A., K. Didan, T. Miura, E.P. Rodriguez, X. Gao, L.G. Ferreira (2002) Overview of the radiometric and biophysical performance of the MODIS vegetation indices. Remote sensing of environment, 83(1-2), 195-213. https://doi.org/10.1016/S0034-4257(02)00096-2

IPCC (2018) Global warming of 1.5°C. An IPCC Special Report on the impacts of global warming of 1.5°C above pre-industrial levels and related global greenhouse gas emission pathways, in the context of strengthening the global response to the threat of climate change, sustainable development, and efforts to eradicate poverty [V. Masson-Delmotte, P. Zhai, H. O. Pörtner, D. Roberts, J. Skea, P.R. Shukla, A. Pirani, W. Moufouma-Okia, C. Péan, R. Pidcock, S. Connors, J. B. R. Matthews, Y. Chen, X. Zhou, M. I. Gomis, E. Lonnoy, T. Maycock, M. Tignor, T. Waterfield (eds.)]. Intergovernmental Panel on Climate Change.

Jenkins L.K., Barry, T., Bosse, K., Currie, W., Christensen, T., Longan, S., Shuchman, R., Tanzer, D., Taylor, J. (2019) Satellite-based Decadal Change Assessments of Pan-Arctic Environments. AMBIO: A Journal of the Human Environment (In press).

Jia, G.J., Epstein, H.E., Walker, D.A. (2009) Vegetation greening in the Canadian Arctic related to decadal warming. Journal of Environmental Monitoring, 11(12), pp.2231-2238.
Jia, G.J., H.E. Epstein, and D.A. Walker. 2003. Greening of arctic Alaska, 1981-2001. Geophysical Research Letters, 30: 2067, https://doi.org/10.1029/2003GL018268

Karami, M., B.U. Hansen, A. Westergaard-Nielsen, J. Abermann, M. Lund, N.M. Schmidt, B. Elberling (2017) Vegetation phenology gradients along the west and east coasts of Greenland from 2001 to 2015. Ambio, 46(1), 94-105. https://doi.org/10.1007/s13280-016-0866-6

Kaufman, D.S., D.P. Schneider, N.P. McKay, C.M. Ammann, R.S. Bradley, K.R. Briffa, K.R., Miller, G.H., Otto-Bliesner, B.L., Overpeck, J.T., Vinther, B.M., Lakes, A. (2009) Recent warming reverses long-term arctic cooling. Science, 325(5945): 1236-1239.
https://doi.org/10.1126/science.1173983

Laidler, G.J., P.M. Treitz, D.M. Atkinson (2007) Remote sensing of arctic vegetation: Relations between the NDVI spatial resolution and vegetation cover on Boothia Peninsula, Nunavut. Arctic, 61(1): 1-13.

Lambert, J., C. Drenou, J.P. Denux, G. Balent, V. Cheret (2013) Monitoring forest decline through remote sensing time series analysis. GIScience & remote sensing, 50(4), 437-457.
https://doi.org/10.1080/15481603.2013.820070

Lanzante, J.R. (1996) Resistant, robust and non-parametric techniques for the analysis of climate data: Theory and examples, including applications to historical radiosonde station data. International Journal of Climatology: A Journal of the Royal Meteorological Society, 16(11),

1197-1226. https://doi.org/10.1002/(SICI)1097-0088(199611)16:11<1197::AID-JOC89>3.0.CO;2-L

Loboda, T.V., J.V. Hall, A.H. Hall, V.S. Shevade (2017) ABoVE: Cumulative Annual Burned Area, Circumpolar High Northern Latitudes, 2001-2015. ORNL DAAC, Oak Ridge, Tennessee, USA, retrieved 1 December, 2016, from https://doi.org/10.3334/ORNLDAAC/1526

McDonald, K.C., J.S. Kimball, E. Njoku, R. Zimmerman, M. Zhao (2004) Variability in springtime thaw in the terrestrial high latitudes: Monitoring a major control on the biospheric assimilation of atmospheric with spaceborne microwave remote sensing. Earth Interactions, 8(2004). https://doi.org/10.1175/1087-3562(2004)8<1:VISTIT>2.0.CO;2

Meltofte, H. (ed.) (2013) Arctic Biodiversity Assessment. Status and trends in Arctic biodiversity. Conservation of Arctic Flora and Fauna, Akureyri, Iceland.

O'Malley, R. (2017) Ocean Productivity. Retrieved December 1, 2018, from http://science.oregonstate.edu/ocean.productivity/index.php

Park, T., Ganguly, S., Tømmervik, H., Euskirchen, E.S., Høgda, K.A., Karlsen, S.R., Brovkin, V., Nemani, R.R., Myneni, R.B. (2016) Changes in growing season duration and productivity of northern vegetation inferred from long-term remote sensing data. Environmental Research Letters, 11. https://doi.org/10.1088/1748-9326/11/8/084001

Parkinson, C.L., D.J. Cavalieri, P. Gloersen, H.J. Zwally, J.C. Comiso (1999) Arctic sea ice extents, areas, and trends, 1978-1996. Journal of Geophysical Research, 104(9): 20837-20856. https://doi.org/10.1029/1999JC900082

R Core Team (2015) R: A language and environment for statistical computing. R Foundation for Statistical Computing, Vienna, Austria, retrieved 1 December, 2016, from https://www.R-project.org/.

Reichle, L.M., H.E. Epstein, U.S. Bhatt, M.K. Raynolds, D.A. Walker (2018) Spatial heterogeneity of the temporal dynamics of Arctic tundra vegetation. Geophysical Research Letters, 45(17): 9206-9215. https://doi.org/10.1029/2018GL078820

Riggs, G.A., D.K. Hall (2016) MODIS Snow Products Collection 6 User Guide. https://nsidc.org/sites/nsidc.org/files/files/MODIS-snow-user-guide-C6.pdf

Riordan, B., D. Verbyla, A.D. McGuire (2006) Shrinking ponds in subarctic Alaska based on 1950–2002 remotely sensed images. Journal of Geophysical Research, 111: G04002, https://doi.org/10.1029/2005JG000150

Smith, L.C., Y. Sheng, G.M. MacDonald, L.D. Hinzman (2005) Disappearing arctic lakes. Science, 308(5727): 1429. https://doi.org/10.1126/science.1108142

Stow, D.A., A.S. Hope, T.H. George (1993) Reflectance characteristics of arctic tundra vegetation from airborne radiometry. International Journal of Remote Sensing, 14(6): 1239-1244. https://doi.org/10.1080/01431169308904408

Stow, D.A., Hope, A., McGuire, D., Verbyla, D., Gamon, J., Huemmrich, F., Houston, S., Racine, C., Sturm, M., Tape, K. Hinzman, L. (2004) Remote sensing of vegetation and land-cover change in arctic tundra ecosystems. Remote Sensing of Environment, 89(3): 281-308. https://doi.org/10.1016/j.rse.2003.10.018

Stroeve, J., W. Meier (2017) Sea Ice Trends and Climatologies from SMMR and SSM/I-SSMIS, Version 2. ESMR-SMMR-SSM/I-SSMIS-Merged Sea Ice Extent. Boulder, Colorado USA. NASA National Snow and Ice Data Center Distributed Active Archive Center, retrieved 1 December, 2016, from http://dx.doi.org/10.5067/EYICLBOAAJOU.

Verbesselt, J., R. Hyndman, A. Zeileis, D. Culvenor (2010) Phenological change detection while accounting for abrupt and gradual trends in satellite image time series. Remote Sensing of Environment, 114(12): 2970-2980. https://doi.org/10.1016/j.rse.2010.08.003.

Watts, J.D., J.S. Kimball, L.A. Jones, R. Schroeder, K.C. McDonald (2012) Satellite microwave remote sensing of contrasting surface water inundation changes within the arctic-boreal region. Remote Sensing of Environment, 127: 223-236. https://doi.org/10.1016/j.rse.2012.09.003

Westermann, S., M. Langer, J. Boike (2011) Systematic bias of average winter-time land surface temperatures inferred from MODIS at a site on Svalbard, Norway. Remote Sensing of Environment, 118, 162–167, 2011. https://doi.org/10.1016/j.rse.2011.10.025

Zeng, H., G. Jia, B.C. Forbes (2013) Shifts in Arctic phenology in response to climate and anthropogenic factors as detected from multiple satellite time series. Environmental Research Letters, 8(3), 035036. https://doi.org/10.1088/1748-9326/8/3/035036

Zeng, H., G. Jia, H. Epstein, H. (2011) Recent changes in phenology over the northern high latitudes detected from multi-satellite data. Environmental Research Letters, 6(4), 045508. https://doi.org/10.1088/1748-9326/6/4/045508

Chapter III

Development of Methods for Detection and Monitoring of Fire Disturbance in the Alaskan Tundra Using a Two-decade Long Record of Synthetic Aperture Radar Satellite Images[3]

Abstract

Using the extensive archive of historical ERS-1 and -2 synthetic aperture radar (SAR) images, this analysis demonstrates that fire disturbance can be effectively detected and monitored in high northern latitudes using radar technology. A total of 392 SAR images from May to August spanning 1992-2010 were analyzed from three study fires in the Alaskan tundra. The investigated fires included the 2007 Anaktuvuk River Fire and the 1993 DCKN178 Fire on the North Slope of Alaska and the 1999 Uvgoon Creek Fire in the Noatak National Preserve. A 3 dB difference was found between burned and unburned tundra, with the best time for burned area detection being as late in the growing season as possible before frozen ground conditions develop. This corresponds to mid-August for the study fires. In contrast to electro-optical studies from the same region, measures of landscape recovery as detected by the SAR were on the order of four to five years instead of one. This time difference provides more opportunities to detect small fires and account for these events in the fire data record.

[3] A version of this chapter has been published as Jenkins et al. 2014

Introduction

The Arctic is changing at unprecedented rates. The changes in the seasonal timing and decreased duration of frozen conditions combined with increased air temperatures has already manifested itself in visible changes in the Arctic landscape including increased plant productivity (Euskirchen et al. 2009), thermokarst, and drying of lakes (Carroll et al. 2011). Changes in wildfire frequency and severity are suspected but undocumented in the tundra. In boreal ecosystems wildfire has already been documented as increasing in frequency and severity over the last 50 years (Soja et al. 2007). However, the baseline fire regime in the tundra is not well quantified due primarily to the relatively low level of human habitation in Arctic regions, and thus limited fire management and suppression efforts. Historically, resources spent mapping fires have been directly correlated to human presence in the region. In turn, tundra fire records are not maintained to the level they have been in boreal regions (Flannigan 2014). Also contributing to the lack of tundra fire data records is that the optical satellite data record over the Arctic has limitations due to persistent cloud cover, lack of algorithms suitable to detection of burns in tundra, and quick green up of tundra vegetation within one year of fire (Loboda et al. 2013). Additionally, the physical and ecological effects of fire disturbance on the tundra are poorly understood due to the logistical challenges of obtaining field measurements, and especially repeat measurements, in remote locations.

An exception to our limited understanding of fire in the tundra is observations of the 2007 Anaktuvuk River Fire on the North Slope of Alaska. This is the largest fire on record (1,039 km2 burned) for the tundra biome and it doubled the cumulative area burned north of 68°N in that region since 1950 (Hu et al. 2010). This fire has been well-studied (Hu et al. 2010, Bret-

Harte et al. 2013, Jones et al. 2009, Mack et al. 2011), but appears to be a novel expression in the tundra fire record as a fire that started mid-summer (July) and persisted late into the growing season (October) and exhibited greater burn severity than typical tundra fire events (Jones et al. 2009). Alternatively, it has been suggested that with climate change the Anaktuvuk River Fire may represent the new normal (Hu et al. 2010). The Anaktuvuk fire scar is less than a decade old, so many questions on recovery of a large, high-burn-severity tundra fire and long-term landscape change remain unanswered.

It is generally known that the factors affecting fire occurrence and the effects of fire on the landscape differ between the tundra and the more extensively-studied boreal regions. In the tundra, as the boreal region, most fires start as a result of lightning strikes. However, while fire events in the boreal zone are of relatively high frequency (159 year fire return interval for 1860-1919 and 105 years for 1920-2009 (Kasischke et al. 2010)) and can be of very large size (average 203 km2 for high fire years and 78 km2 for low fire years for the period 1950-1999 (Kasischke et al. 2006), in the tundra fire events are generally rare and small in size (Wein and Bliss, 1973)). Historically, tundra fire events have occurred in June and July (Racine et al. 1985), with average size of 30-55 km2 (French et al. 2015) with an estimate of cumulative decadal burning of 744 km2 on the North Slope of Alaska (Rocha et al. 2012).

Several ecoregion (Gallant et al. 1995, Jones et al. 2013, Nowacki,et al. 1995) and vegetation maps (CAVM Team 2003, Raynolds et al. 2006) exist for Alaska and the pan-Arctic that can be used to delineate the geographic extent of tundra. While differences exist in these map products, approximately six ecoregions are covered within tundra vegetation extents in Alaska. These geographic areas include, from north to south: North Slope Coastal Plain, Brooks

Range Foothills, Brooks Range, Kotzebue Lowlands, Seward Peninsula, and Southwest Alaska. Differences in the fire regime between these geographic areas exist (Hu et al. 2010, Rocha et al. 2012, Racine et al. 1987), but despite differences in fire frequency and size, the persistent patterns of vegetation across the different regions may have similar post fire recovery.

There is evidence that climate change has led to an increase in fire occurrence in tundra regions. Hu et al. (2010) show through paleoecological evidence that recent tundra burning is unprecedented in the central Alaska Arctic within the last 5,000 years. Fuel loads (plant biomass) are expected to increase over time in high northern latitudes as shrub dominated land cover increases (Chapin et al. 2005, Tape et al. 2006). These enhanced fuel reserves are likely to result in increased burned area and fire severity which would be detrimental to ecosystem services such as wildlife habitat.

The Alaskan tundra falls within the zone of continuous permafrost. Fire events are known to locally disturb permafrost by increasing the active layer – the depth of seasonal soil thaw. Permafrost recovery is largely a function of vegetation recovery and thus pre-fire vegetation, slope characteristics, and fire characteristics (Racine et al. 2004). Thermokarst occurs through large-scale permafrost degradation, and can significantly alter the local hydrology though the draining and creation of thermokarst lakes (Grosse et al. 2011, Swanson 1996). The extent to which fire increases active layer, thermokarst, and alters surface hydrology in the tundra has not been widely investigated.

Electro-optical and thermal satellite sensors may be used to detect initial changes in temperature and surface composition resulting from a fire event (French et al. 1996). Synthetic

Aperture Radar (SAR) sensors are sensitive to changes in surface roughness and soil moisture, making SAR useful for characterizing longer-term patterns and trends that occur post-fire (Bourgeau-Chavez et al. 1997, Bourgeau-Chavez et al. 2007, Kasischke et al. 1992). In the persistently cloudy and hazy Arctic environments, SAR systems have the added benefit of more useable image observations as compared to electro-optical systems due to all-weather imaging capabilities. SAR data has also proven useful for monitoring other ecological parameters in high northern latitudes (Reschke et al. 2012).

Recent research (Loboda et al. 2013) in the North American tundra using Landsat imagery shows that the electro-optical spectral signature of burned areas deteriorate rapidly, resulting in fire-disturbed sites being poorly distinguishable from unburned tundra by the end of the first post-fire season. In contrast, the remote sensing signature in SAR imagery is likely to be much more long-lived due to the geophysical changes detected with SAR backscatter imagery. Research in the boreal region using SAR data has shown that fire scars are detectable for five to seven years post-fire (Kasischke et al. 1992, Bourgeau-Chavez et al. 1994). In boreal regions fire scars are typically three to six dB brighter than adjacent unburned forests in the spring (May) after snowmelt due to changes in surface roughness, moisture, and removal of tree canopies (Kasischke et al. 1995). The decreased evapotranspiration, thawing of frozen ground and deepening of active layers makes the burned regions wetter than adjacent unburned forests and this is detected by the SAR sensors as enhanced backscatter.

The study presented addresses the hypothesis that the SAR signature from fire-disturbed sites in tundra will persist for several years post-fire, as has been documented in boreal sites. This paper presents a previously undocumented temporal assessment of

radiometric response (i.e. SAR backscatter) captured by the SAR instruments on board the Earth Resources Satellite/European Remote-Sensing Satellite (ERS) at three fire scars in the Alaskan tundra. SAR data are shown to be useful for detection, monitoring, and quantifying temporal changes in fire disturbed landscapes. The goal of this analysis is to assess the landscape response to fire and to quantify the longevity of these effects as observed through radar images.

Materials and Methods

Study Area

The 2007 Anaktuvuk River Fire, the 1999 Uvgoon Creek Fire, and the 1993 DCKN178 Fire are the focus of this analysis (Figure 1, Table 1). These tundra fires were selected to cover a range of large, medium, and small fire sizes. These fires were also selected based upon the year of burn with respect to the two-decade long radar satellite record to include fire events early, mid, and late in the data record. Inclusion of these fires also provided examples from both the Noatak National Preserve and the North Slope of Alaska.

All three fires are located in the same Foothills Ecoregion as defined by the EcoMap data layer (Nowacki and Brock 2001), but the Anaktuvuk River and the DCKN178 Fires are located north of the Brooks Range on the North Slope and the Uvgoon Creek Fire is located south of the Brooks Range in the Noatak National Preserve. All of the fires burned for a long time (more than one month, see Table 1) and the Uvgoon Fire burned the earliest within the growing season based on the date of completed burning. The Anaktuvuk River Fire burned the latest into the growing season but also burned the longest, and portions of this fire could be representative of

different burning conditions. All three fires occurred on relatively flat terrain with the burned area constrained primarily by river and stream features. The general vegetation types found in the three study areas are similar, with a dominate cover type of tussock tundra or tussock-shrub tundra (Boggs et al. 2012) with the difference being the percentage of shrub, typically greater than or less than 25%. The land cover data layers for this region aren't suitable for a detailed comparison among the study sites, but vegetation is relatively homogeneous in this region and should affect post-fire dynamics similarly.

Table 3-1. *The Anaktuvuk River Fire, DCKN178 Fire, and Uvgoon Creek Fire are the focus of this analysis. These fires provide examples of small, medium, and large fire sizes for the tundra biome. These fires also burned at different times within the two-decade ERS satellite data record providing different pre-burn and post-burn lengths of observations.*

Fire	**Year of Burn**	**Fire Duration**	**Fire Size**	**Area Burned (km^2)**	**Location**	**Years of ERS SAR Data Available**
Anaktuvuk River	2007	July 16 - October 9	Large	1,039	North Slope Foothills	15 pre-burn/ 3 post-burn
Uvgoon Creek	1999	June 26 - August 3	Medium	359	Noatak National Preserve	7 pre-burn/ 11 post-burn
DCKN178	1993	July 9 - August 17	Small	68	North Slope Foothills	1 pre-burn/ 16 post-burn

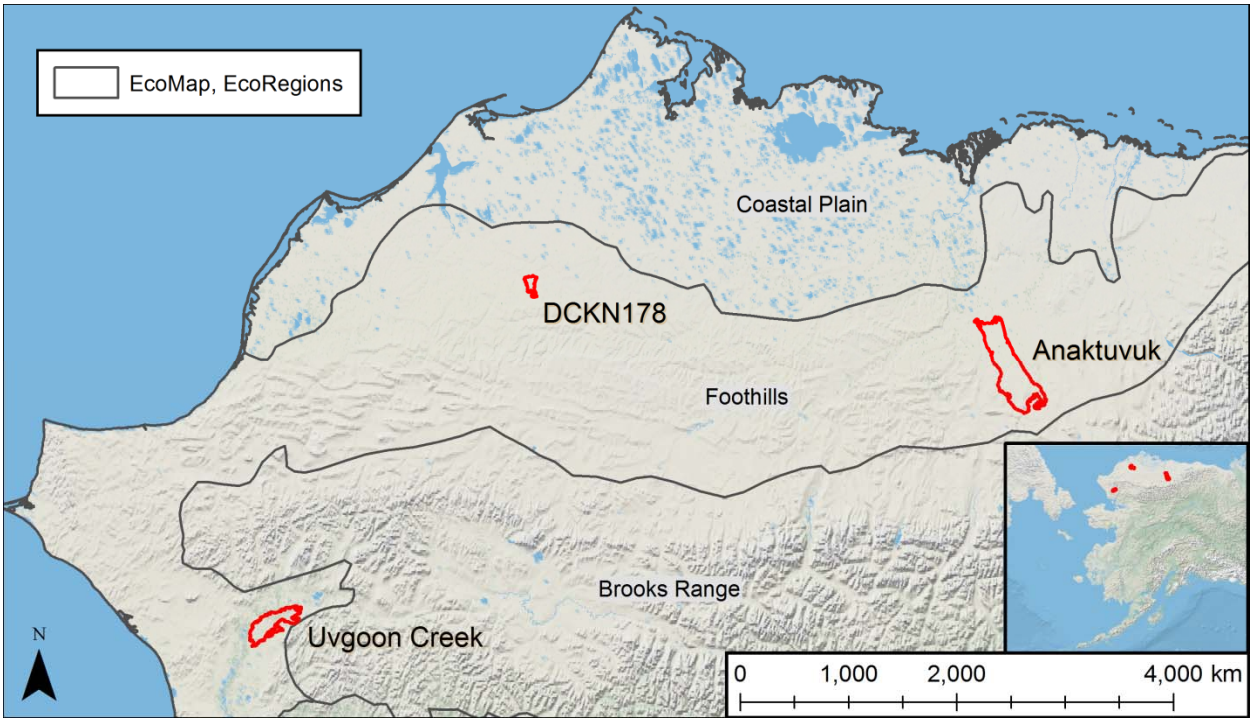

Figure 3-1. *The Anaktuvuk River, Uvgoon Creek, and DCKN178 Fires are all located in the Foothills Ecoregion as defined by the EcoMap data layer (Nowacki and Brock 1995), the Anaktuvuk River and DCKN178 Fires are located north of the Brooks Range and the Uvgoon Creek fire is located south of the Brooks Range.*

Ancillary and Remote Sensing Data

Fire scar polygons were initially obtained from the Alaska Large Fire Database (Kasischke et al. 2002) available through the Alaska Interagency Coordination Center (AICC; http://fire.ak.blm.gov/). Using post-fire Landsat and SAR scenes the accuracy of the AICC polygons were evaluated. The accuracy of the scars perimeters varied strongly: the Uvgoon Creek Fire perimeter was mapped very accurately whereas DCKN178 perimeter required extensive updates and corrections. Updated and more accurate perimeters were hand-digitized from Landsat imagery for the Uvgoon Creek (path 81, row 12, August 8, 1999) and Anaktuvuk River (path 75, row 11, June 15 2008) Fires. ERS data (E1_15352_STD_F275, June 22, 1994)

were used to update the DCKN178 fire as cloud-free, one-year-post-fire Landsat image scene was not available.

Homogeneous paired polygon sample areas within the burn and in adjacent unburned areas were delineated to use for analysis to investigate temporal trends within each polygon and spatial homogeneity or heterogeneity of backscatter response across the landscape. Polygon samples of 6 km^2 minimum size were placed to represent the geographic extents of the fire scars and to provide averaging areas to account for speckle. Three polygon pairs were selected for the Anaktuvuk and Uvgoon Fires due to their large and medium fire size, respectively. Two polygon pairs were selected for the smaller DCKN178 Fire.

Pre-burn and post-burn satellite images, land cover and vegetation maps, and hydrology and elevation data layers were used to select the location of the polygon pairs. The goal of the image analysis was to remove any difference between the burn and unburned areas within each pair other than the burn status. Unburned areas in the images were selected to best match pre-burn conditions within each pair with respect to land cover classification maps, texture, tone, and landscape context (i.e. elevation and hydrology). Given the complexity of the landscape in respect to hydrologic features in all fires, fire history and topographical constraints for the Uvgoon fire, and the location of the SAR image edge in respect to the fire scar, there were limited options available for polygon placement. The size and shapes of the polygons were dedicated by the spatial complexity of the landscape and the size and shape of the fire scars. Narrow polygons were used for Uvgoon to avoid the many small kettle lakes ringed by trees within the fire scar that were not prevalent outside the fire scar. Less spatial variation existed between burned and unburned polygon pairs in the Anaktuvuk and DCKN178 fires so wider

rectangles were used. Any small-scale variation within the polygonswas accounted for in the large size of the polygons and spatial averaging of many pixels. A map of the digitized polygons and the fire scars overlaid on an August SAR image one year post fire is shown in Figure 2.

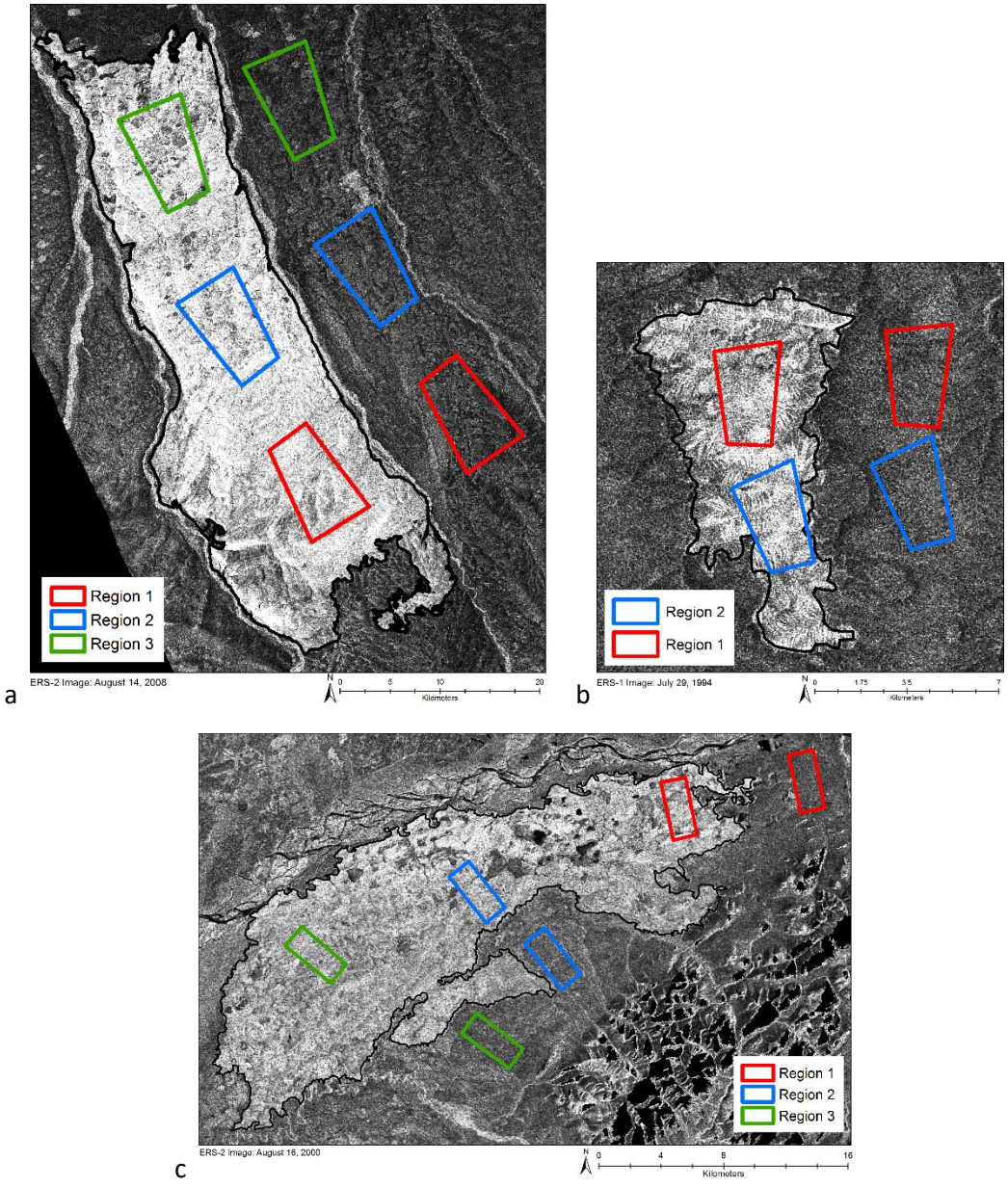

Figure 3-2. *Post-burn ERS SAR images show higher backscatter vales (brighter) of the burned areas versus the surrounding landscape. The regions used in the ANOVA effects model and defined by the homogeneous burned and unburned polygon pairs for Anaktuvuk River Fire (a), DCKN178 Fire (b), and Uvgoon Creek Fire (c) are shown on ERS images one year post fire. The updated fire scar polygons are also shown in black.*

SAR data from the ERS-1 and -2 (C-band, VV-polarization) were used to quantify the radiometric response at the three study locations. The ERS-1 satellite was in operation from July 17, 1991 to March 10, 2000. The ERS-2 satellite was operational April 21, 1995 to September 5, 2011. All images from May to August of each year spanning the available data record from 1992-2010 were obtained to generate a nineteen year dataset. A total of 392 images were analyzed (194 from Anaktuvuk, 101 from DCKN178, and 97 from Uvgoon). Out of the 392 scenes, 279 images were acquired between June and August (the months used for statistical analysis) and the availability by fire for each year is outlined in Table 2.

Image Processing and Analysis

All images were obtained from the Alaska Satellite Facility and processed using their MapReady Software (version 3.2.1). Data processing included conversion of level 1 detected data to radar cross-section (σ°) with gain correction applied to the ERS-2 data. Terrain correction and geocoding to UTM, WGS84 using a bilinear resampling method were applied using the MapReady software and images were exported as GeoTIFFs. The radiometric accuracy for ERS-1 is -0.49 dB and -1.64 dB for ERS-2 (Albright 2000).

Average radiometric response within each polygon for a given image scene was calculated with the Zonal Analysis tool in ArcGIS. GIS and statistical analysis was performed on the σ° data. Data were then converted to dB for visualization and reporting using the following equation:

$$dB = 10 * log_{10}\sigma^{\circ}$$

Approximately four to five image scenes were available for each year from May to August (Table 2). No image scenes were available in 1996 for DCKN178 and 1997 for Uvgoon. Initial data exploration showed variable radiometric response in May among the different fires and years (see Results section), therefore we limited the statistical analysis to include only data values from June to August. Data for each polygon from each image scene within a given year were averaged to obtain one value per polygon per year.

Table 3-2. *A total of 279 ERS-1 and -2 image scenes from June through August from 1992-2010 were used to conduct the statistical analysis. Image availability by fire and year is documented in this table.*

	1992	1993	1994	1995	1996	1997	1998	1999	2000	2001	2002	2003	2004	2005	2006	2007	2008	2009	2010
Anaktuvuk	6	5	5	10	1	3	2	6	8	6	6	7	10	10	11	12	9	7	8
DCKN178	5	4	4	5	0	4	4	7	4	1	3	2	2	4	4	4	4	4	6
Uvgoon	5	5	2	4	2	0	3	7	5	5	6	4	3	4	4	3	5	6	3

Analysis of variance (ANOVA) was used to conduct a longitudinal analysis of landscape recovery post-fire. A three-way additive effects ANOVA was implemented for each fire that estimates σ° as a function of the year in which burn occurred (the year effect), the polygon regions (the region effect), and burn status (the burn effect).

The model developed for the data is:

$$X_{ijk} = \mu_i + \alpha_j + \varepsilon_{ijk} \qquad k = 1, i = 1,2, \dots, 19, j = 1,2,3$$

$$X_{ijk} = \mu_i + \alpha_j + \varepsilon_{ijk} \qquad k = 1, i = 1,2, \dots, i_b, j = 1,2,3$$

$$X_{ijk} = \mu_i + \alpha_j + \nu_i + \varepsilon_{ijk} \qquad k = 2, i = i_b, i_b + 1, \dots, 19, j = 1,2,3$$

Where:

$i = \text{year}$

$j = \text{region}$

$k = \text{index for unburned (k = 1)and burned (k = 2)}$

$i_b = \text{year in which burn occured}$

$\mu_i = \text{year effect}$

$\alpha_j = \text{region effect}$

$\nu_i = \text{burn effect}$

$\varepsilon_{ijk} = \text{error} \sim \text{normally distributed with variance } \sigma^2$

Given the data model, the three-way ANOVA model is of the form:

$$Y_{ijl} = \mu_i + \alpha_j + \nu_{l,i}$$

Where l = 0 if unburned and l = 1 corresponds to burned, and

$$\nu_{l,i} = 0 \qquad l = 0$$

$$\nu_{l,i} = \nu_i 0 \qquad l = 1, i \geq i_b$$

To explore the effect of the different regions on the effect of burn, Tukey Honest Significant Differences (HSD) tests were performed for each fire.

Results

Recent tundra fire scars appear brighter (higher backscatter values) in the SAR images than the surrounding landscape (Figure 2). Typically, fire scars are brightest one year post fire with the brightness gradually decreasing each subsequent year post-fire. The fires evaluated are approximately 3.0 to 3.3 dB brighter than adjacent unburned areas during the end of the growing season one year post fire. For the Anaktuvuk and Uvgoon datasets the difference between burned and unburned is smaller (0.1 to 0.6 dB) in early May, with the difference increasing over the growing season, and reaching a maximum in early to mid-August (Figure 3). This trend cannot be evaluated in the DCKN178 plot (Figure 2), because May and August data were not available one year after the fire event. Generally, the May data for all three fires showed variable response year-to-year but May images consistently showed less differentiation between burned and unburned signatures.

Plots of the radiometric response over the entire ERS data record (Figure 4) clearly show the fire event (dashed line in Figure 4 plots) and the lasting impact on the record. Visual inspection of the plots shows the divergence in the burned versus unburned series that persists for approximately four to five years post fire for all three scenarios. The Uvgoon fire generally has higher and more stable backscatter values than the Anaktuvuk and DCKN178 fires. The Uvgoon data record shows dB values in the range on -6 to -11 with the approximately 3 dB separation in the burned versus unburned polygons. The North Slope fires, Anaktuvuk and DCKN178, have backscatter values in the range of -6 to -17 dB with a decreasing trend over time. The fire event is again clearly visible in these temporal plots.

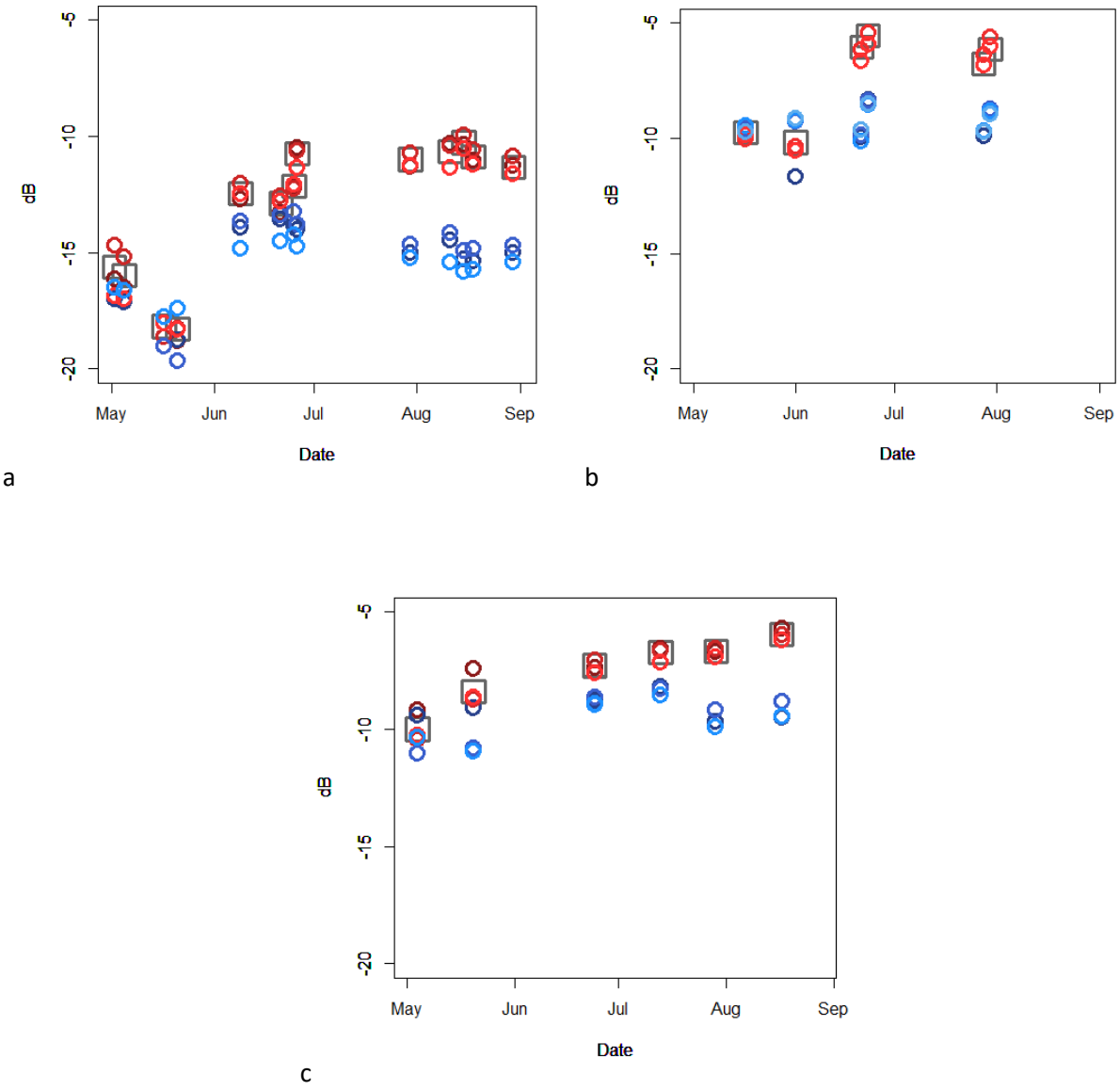

Figure 3-3. *Intra-annual plots of May through August backscatter one year post fire within the entire burn perimeter (grey square) and polygon pairs (red corresponds to burn and blue to unburned) show maximum differentiation between burned and unburned area approximately mid-August for Anaktuvuk (a) and Uvgoon (c). Data are not available in May or August one year post-fire for DCKN178 (b)*

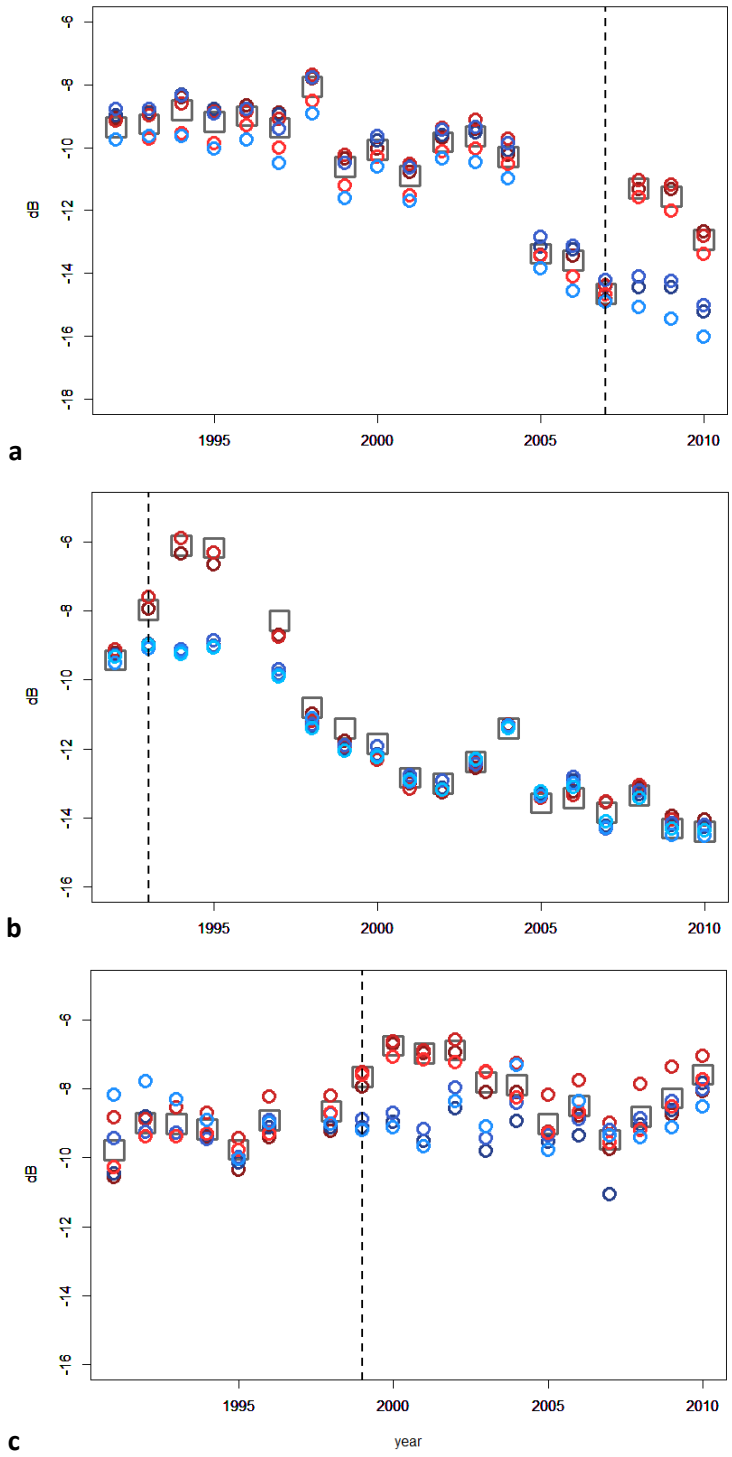

Figure 3-4. *Plots of the backscatter response over time for the entire ERS-1 and -2 data record. The dashed line shows the fire event within the data record. Burned polygons are represented with red markers and unburned polygons with blue. Points represent averaged data from June, July, and August. Note the long-term, downward trend in the DCKN178 (b) and Anaktuvuk (a) plots that is occurring irrespective of the fire event. This trend is not evident in the Uvgoon (c) plot. This may indicate an overall regional trend, such as drying, for the North Slope of Alaska that is not occurring elsewhere.*

The ANOVA results show approximately four to five years are needed for landscape recovery, as defined by a return to the pre-fire signature, of burned areas in the SAR imagery. Plots of the burn years versus the effect of burn for each fire (Figure 5) show a return to zero effect, within the 95% confidence envelope, at 2004 (five years post fire) for Uvgoon Creek and at 1998 (four years post fire) for DCKN178. The Anaktuvuk River Fire does not return to zero effect of burn given the available data, but 2008, 2009, and 2010 (three years post fire) are all above the zero effect line.

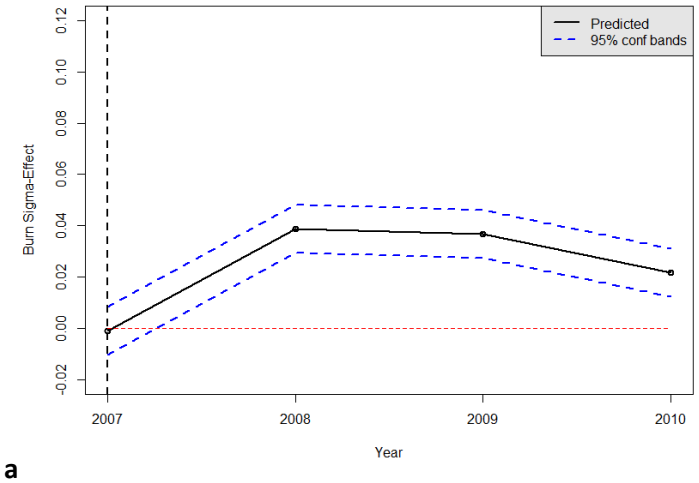

a

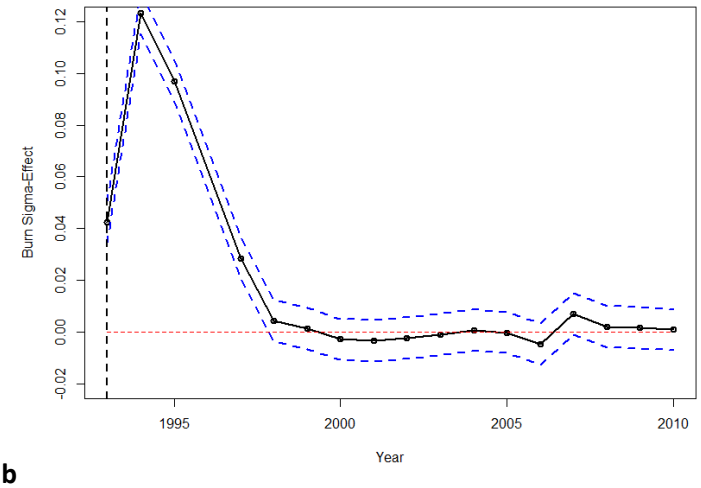

b

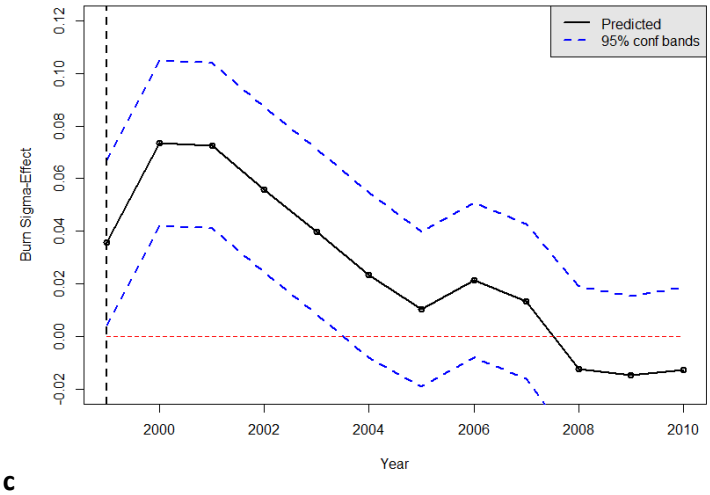

c

Figure 3-5. *Plots of the effect of burn derived from the ANOVA model show landscape recovery (a return to zero burn effect) four years post-fire for DCKN178 (b) and five years post-fire for Uvgoon (c). Not enough data are available to document the return for the Anaktuvuk River Fire (a), but three years post fire is above the zero-effects line. The 95% confidence intervals are represented by the dashed blue lines and the fire year is shown by the dashed black lines.*

The Tukey HSD tests were implemented to investigate if differences existed in the means of the different regions within each burn. The results were variable and did show some regional effects for the Anaktuvuk and Uvgoon Creek Fires. No significant difference between regions 1 and 2 ($p=0.097$) were found for the DCKN178 Fire. For the Anaktuvuk River Fire no difference was found between regions 1 and 2 ($p=0.428$) but statistically significant differences were found between region 3 and regions 1 and 2 ($p < 0.001$ for both). For the Uvgoon Creek Fire no significant difference was detected between region 2 and 3 ($p=0.956$) but a significant difference between region 1 and regions 2 and 3 ($p=0.001$ and $p=0.004$, respectively) was observed.

Table 3-3. *The p-values from the Tukey HSD test show Region 3 from Anaktuvuk and Region 1 from Uvgoon (Figure 2) are statistically different from the other regions within these fires.*

DCKN178			
	Region 1	Region 2	
Region 1			
Region 2	0.097		
Anaktuvuk River			
	Region 1	Region 2	Region 3
Region 1			
Region 2	0.428		
Region 3	< 0.001*	< 0.001*	
Uvgoon Creek			
	Region 1	Region 2	Region 3
Region 1			
Region 2	0.001*		
Region 3	0.004*	0.956	

Discussion

Previous research in boreal forests found a three to six dB difference in ERS SAR backscatter in burned versus unburned sites. In this analysis of tundra fire sites a three dB difference has been detected for the tundra sites studied. A 1994 boreal wildfire near Gerstle River, Alaska had average ERS-1 backscatter of -4.5 dB compared to -8 to -10 dB (3.5 to 5.5 dB difference) for adjacent unburned forests in the spring of 1995 (one year post-burn). This compares to the 1993 DCKN178 fire which had peak backscatter in late-July 1994 of -6 dB and the adjacent unburned tundra had on average -9 dB backscatter (3 dB difference). The effects of standing dead trees in burned boreal forests was at first thought to be causing a double bounce (enhanced backscatter) effect. However, the effects of the trees was determined as negligible due to low moisture content of the boles; instead surface roughness was determined to be the greatest factor, coupled with high moisture content, in causing the bright backscatter return from burned boreal forests (Bourgeau-Chavez et al. 2002). Similarly, in the tundra the C-band energy is scattering from the rough ground surface causing an enhanced signature when the ground is wet. Distinctions between tundra and boreal that could affect the backscatter differences between burned and unburned areas of these two ecoregions include greater variation in vegetation structure and composition pre-fire in boreal, differences in seasonal timing of ground thaw, greater severity of burning within duff and organic layers in boreal, slow post-burn vegetation recovery in boreal versus tundra, shallower active layer and organic soil depths in the tundra. Further investigation into the dominant scattering mechanisms, surface roughness conditions, and seasonal trends in soil moisture are needed in the tundra and boreal to fully understand the differences observed by the C-band sensors.

Intra-annual observations in the years post fire reveal a greater separation in backscatter values as the growing season progresses. Differences in springtime (May) were found to be very low, most likely due to frozen ground conditions. For this reason, May data were omitted from the statistical analysis. Peak differentiation between burned and unburned polygons was found late-July to mid-August, depending on image availability. Wetness increases during the growing season due to permafrost thaw and reaches a peak in mid-August when active layer measurements are typically taken. This shows that the best time to detect fire scars in the Arctic is as late in the growing season as possible before frost and frozen ground conditions develop. For the North Slope and Noatak National Preserve study regions this corresponds to mid-August.

The Anaktuvuk River Fire was a much larger fire than DCKN178 or Uvgoon, which accounts for the larger range of variability in polygon backscatter signatures for Anaktuvuk. North to south, the Anaktuvuk fire scar spans different topography, types and proportions of land cover classes, as well as differences in hydrology which all affect the observed backscatter. Similarly, Uvgoon is larger than DCKN178 and thus displays a larger range of backscatter values.

The results from the ANOVA effects model show landscape recovery, as detected by statistically significant changes in backscatter, 4-5 years post-fire. This means there is a 4-5 year window to detect burned areas in the tundra, and a comprehensive mapping effort using SAR data could be conducted every 4-5 years and theoretically map all fires that occurred during this the previous 4-5 year time period. These results show that the landscape is affected over a longer period of time than is observed through electro-optical satellite data. Previous electro-optical studies (Loboda et al. 2013) show recovery as early as late season for early season burns

(less than one year) and one year post fire. Electro-optical and microwave sensors are detecting different landscape parameters. Measures of electro-optical recovery are mainly detecting changes in vegetation and vegetation greenness; whereas SAR sensors are detecting moisture and surface roughness changes post-fire. Further research is needed to better develop the relationships between soil moisture and surface roughness on the detected backscatter over time.

Visual observations of the individual SAR images show the persistence of the fire scar longer than the four to five years as detected though statistical means. Based on our experience with these three fires, the human eye can detect the diminishing fire scar up to ten years post fire, although admittedly, the remnant signature is patchy and only small portions remain discernable. This is comparable to research results as reported in boreal systems, accounting for differences in methodology and number of SAR images analyzed. It is also interesting to note that visual observation of the individual ERS image scenes for the three fires do not show any progression of the fire scar boundary over time. It was initially hypothesized that the fire could affect the radar response directly adjacent and outside the burn perimeter due to melting of permafrost and other hydrologic changes from the fire, but this does not appear to occur at the three fires investigated.

The result of the investigation into regional effects within each fire is not surprising given the size of the three different test fires. No regional effects were observed in the smallest fire, DCKN178. Regional effects were found at the medium and large fires, Uvgoon and Anaktuvuk, but in both scenarios, only one of the three regions was statistically different from the other two. For the Anaktuvuk Fire the far northern polygons (Figure 2) correspond to the

statistically different region. They may be the result of different land cover or vegetation types in this region or the topographical position on the landscape. The far northern polygons also have a higher percentage of surface water features and may have higher soil moisture values which could be introducing increased intra- and inter-annual variability in the backscatter values for these regions. For the Uvgoon Creek fire, the polygon pairs in the far western portion (Figure 2) of the overall fire scar correspond to the statistically different region. The available ancillary data layers for this region do not reveal the same noteworthy differences as were found for Anaktuvuk, but the p-values were not as small as were found at Anaktuvuk either. The results for the three fires show that spatial autocorrelation does affect the radiometric response, and provides evidence for developing different regional models for large fire sizes. This is most likely not necessary for small fires, given the observations from this study.

The Noatak and the North Slope fires display a difference in radiometric response over time. Regardless of the timing of the fire event within the radar data record, the Noatak trend is relatively stable over time, but the North Slope sites show a general downward trend over time. This finding is significant and may indicate regional drying that is occurring on the North Slope but not in the Noatak (Bourgeau-Chavez et al. in prep). Further test areas distributed across the North Slope and both north and south of the Brooks Range are needed in combination with in situ measurements to further investigate this finding.

Conclusions

SAR is powerful tool for fire detection and fire effects monitoring in the Arctic. Persistent cloud-cover and haze severely limits electro-optical satellite applications in this

region. SAR data can be used to provide image looks when electro-optical data are not available, and integration of SAR data within current fire detection algorithms could increase the number of detections. The fire perimeter for the DCKN178 fire was not accurate in the AICC Alaska Large Fire Database potentially due to the lack of cloud-free Landsat data one year post-fire. SAR image data could be used to generate perimeters, and thus area estimates, of burned areas in the tundra as was demonstrated as feasible in boreal regions [30, 35]. Increased fire detections and more accurate estimates of area burned would provide the data for better characterization of the baseline fire regime in this region. Without accurate baseline data it is difficult, if not impossible, to determine if fire regime is changing in the Arctic and the extent to which ecosystem services are affected. Improved baseline data is also needed to refine fire emissions estimates and carbon accounting.

Electro-optical and radar sensors are measuring different landscape parameters and SAR data can be used to detect additional and complementary information to what can be extracted from optical systems. Within the wildfire community, algorithms currently exist to map burn severity and the inclusion of SAR data within these algorithms may provide better correlation between satellite and in situ data and result in more accurate map outputs. Other research fields that could benefit from inclusion of SAR wildfire monitoring data are studies in permafrost and surface hydrology. Algorithm development estimating active layer depth as a function of backscatter would be beneficial to many stakeholders beyond the wildfire community, but fire events provide opportunities for detection and monitoring of rapid changes and recovery that typically are not available within baseline studies.

Two decades of ERS SAR data are available in the data archive, but no new images are being acquired. This analysis could be extended with the inclusion of both archive and new data from of other satellite SAR systems. C-band archive data from Radarsat-1 and 2 and Envisat exist, and new data requests can be submitted for Radarsat-2. Additionally, the Sentinal-1 mission is planned for launch in 2014 and is designed to provide C-band data continuity building on the legacy of ERS, Envisat, and Radarsat. A constellation of Radarsat-2 satellites is also planned and could provide additional data options.

References

Albright, W. (2000) Calibration Report for ERS-1 and ERS-2 on the Precision Processor. Alaska Satellite Facility: Fairbanks, AK, USA.

Boggs, K., Boucher, T. V., Kuo, T. T., Fehringer, D., Guyer, S. (2012) Vegetation map and classification: Northern, western and interior Alaska. Anchorage: Alaska Natural Heritage Program, University of Alaska.

Bourgeau-Chavez, L. L., Kasischke, E. S., Riordan, K., Brunzell, S., Nolan, M., Hyer, E., Slawski, J., Medvecz, M., Walters, T., Ames, S. (2007) Remote monitoring of spatial and temporal surface soil moisture in fire disturbed boreal forest ecosystems with ERS SAR imagery. International Journal of Remote Sensing, 28(10), 2133-2162.

Bourgeau-Chavez, L. L., Kasischke, E. S., Brunzell, S., Mudd, J. P., Tukman, M. (2002) Mapping fire scars in global boreal forests using imaging radar data. International Journal of Remote Sensing, 23(20), 4211-4234.

Bourgeau-Chavez, L. L., Harrell, P. A., Kasischke, E. S., French, N. H. F. (1997) The detection and mapping of Alaskan wildfires using a spaceborne imaging radar system. International Journal of Remote Sensing, 18(2), 355-373.

Bourgeau-Chavez, L. L. (1994) Using ERS-1 SAR imagery to monitor variations in burn severity in an Alaskan fire-disturbed boreal forests. Doctoral dissertation, University of Michigan.

Bret-Harte, M. S., Mack, M. C., Shaver, G. R., Huebner, D. C., Johnston, M., Mojica, C. A., Pizano, C., Reiskind, J.A. (2013) The response of Arctic vegetation and soils following an unusually severe tundra fire. Philosophical Transactions of the Royal Society B: Biological Sciences, 368(1624), 20120490.

Carroll, M. L., Townshend, J. R. G., DiMiceli, C. M., Loboda, T., Sohlberg, R. A. (2011) Shrinking lakes of the Arctic: Spatial relationships and trajectory of change. Geophysical Research Letters, 38(20).

CAVM Team (2003) Circumpolar Arctic Vegetation Map. In Conservation of Arctic Flora and Fauna (CAFF) Map No. 1, U.S. Fish and Wildlife Service: Anchorage, Alaska.

Chapin, F. S., Sturm, M., Serreze, M. C., McFadden, J. P., Key, J. R., Lloyd, A. H., McGuire, A.D., Rupp, T.S., Lynch, A.H., Schimel, J.P., Beringer, J. (2005) Role of land-surface changes in Arctic summer warming. Science, 310(5748), 657-660.

Euskirchen, E. S., McGuire, A. D., Chapin III, F. S., Yi, S., Thompson, C. C. (2009) Changes in vegetation in northern Alaska under scenarios of climate change, 2003–2100: implications for climate feedbacks. Ecological Applications, 19(4), 1022-1043.

Flannigan, M. (2014) Personal correspondence.

French, N. H., Jenkins, L. K., Loboda, T. V., Flannigan, M., Jandt, R., Bourgeau-Chavez, L. L., Whitley, M. (2015) Fire in arctic tundra of Alaska: past fire activity, future fire potential, and significance for land management and ecology. International journal of wildland fire, 24(8), 1045-1061.

French, N. H. F., Kasischke, E. S., Johnson, R. D., Bourgeau-Chavez, L. L., Frick, A. L., Ustin, S. L. (1996) Estimating fire-related carbon flux in Alaska boreal forests using multi-sensor remote sensing data. In *Biomass burning and global change*, Levine, J.S., Ed. MIT Press: Cambridge, Mass. pp 808-826.

Gallant, A.L., Binnian, E.F., Omernik, J.M., Shasby, M.B. (1995) Ecoregions of Alaska. U.S. Geological Survey Professional Paper, 1567, 73.

Grosse, G., Harden, J., Turetsky, M., McGuire, A. D., Camill, P., Tarnocai, C., Frolking, S., Schuur, E.A., Jorgenson, T., Marchenko, S., Romanovsky, V. (2011) Vulnerability of high-latitude soil organic carbon in North America to disturbance. Journal of Geophysical Research: Biogeosciences, 116(G4).

Hu, F. S., Higuera, P. E., Walsh, J. E., Chapman, W. L., Duffy, P. A., Brubaker, L. B., Chipman, M. L. (2010) Tundra burning in Alaska: linkages to climatic change and sea ice retreat. Journal of Geophysical Research: Biogeosciences, 115(G4).

Jenkins, L., Bourgeau-Chavez, L., French, N., Loboda, T., Thelen, B. (2014) Development of methods for detection and monitoring of fire disturbance in the Alaskan tundra using a two-decade long record of synthetic aperture radar satellite images. Remote Sensing, 6(7), 6347-6364.

Jones, B. M., Breen, A. L., Gaglioti, B. V., Mann, D. H., Rocha, A. V., Grosse, G., Arp, C.D., Kunz, M.L., Walker, D. A. (2013) Identification of unrecognized tundra fire events on the north slope of Alaska. Journal of Geophysical Research: Biogeosciences, 118(3), 1334-1344.

Jones, B. M., Kolden, C. A., Jandt, R., Abatzoglou, J. T., Urban, F., Arp, C. D. (2009) Fire behavior, weather, and burn severity of the 2007 Anaktuvuk River tundra fire, North Slope, Alaska. Arctic, Antarctic, and Alpine Research, 41(3), 309-316.

Kasischke, E. S., Verbyla, D. L., Rupp, T. S., McGuire, A. D., Murphy, K. A., Jandt, R., Barnes, J.L., Hoy, E.E., Duffy, P.A., Calef, M., Turetsky, M. R. (2010) Alaska's changing fire regime—

implications for the vulnerability of its boreal forests. Canadian Journal of Forest Research, 40(7), 1313-1324.

Kasischke, E. S., Rupp, T. S., Verbyla, D. L. (2006) Fire trends in the Alaskan boreal forest. Alaska's changing Boreal forest, 285-301.

Kasischke, E. S., Williams, D., Barry, D. (2002) Analysis of the patterns of large fires in the boreal forest region of Alaska. International Journal of Wildland Fire, 11(2), 131-144.

Kasischke, E. S., Morrissey, L., Way, J., French, N. H., Bourgeau-Chavez, L. L., Rignot, E., Stearn, J.A., Livingston, G. P. (1995) Monitoring seasonal variations in boreal ecosystems using multi-temporal spaceborne SAR data. Canadian Journal of Remote Sensing, 21(2), 96-109.

Kasischke, E. S., Bourgeau-Chavez, L. L., French, N. H. F., Harrell, P., Christensen Jr, N. L. (1992) Initial observations on using SAR to monitor wildfire scars in boreal forests. International Journal of Remote Sensing, 13(18), 3495-3501.

Loboda, T. V., French, N. H., Hight-Harf, C., Jenkins, L., Miller, M. E. (2013) Mapping fire extent and burn severity in Alaskan tussock tundra: An analysis of the spectral response of tundra vegetation to wildland fire. Remote Sensing of Environment, 134, 194-209.

Mack, M. C., Bret-Harte, M. S., Hollingsworth, T. N., Jandt, R. R., Schuur, E. A., Shaver, G. R., Verbyla, D. L. (2011) Carbon loss from an unprecedented Arctic tundra wildfire. Nature, 475(7357), 489.

Nowacki, G., Brock, T. (1995) Ecoregions and subregions of Alaska, EcoMap Version 2.0 (map). USDA Forest Service, Alaska Region (Juneau, AK).

Nowacki, G., Spencer, P., Fleming, M., Brock, T., Jorgenson, T. (2001) Ecoregions of Alaska: 2001. Open-file report 02-297 (map). US Geological Survey.

Racine, C., Jandt, R., Meyers, C., Dennis, J. (2004) Tundra fire and vegetation change along a hillslope on the Seward Peninsula, Alaska, USA. Arctic, Antarctic, and Alpine Research, 36(1), 1-10.

Racine, C. H., Dennis, J. G., Patterson III, W. A. (1985) Tundra fire regimes in the Noatak River watershed, Alaska: 1956-83. Arctic, 194-200.

Racine, C. H., Johnson, L. A., Viereck, L. A. (1987) Patterns of vegetation recovery after tundra fires in northwestern Alaska, USA. Arctic and Alpine Research, 19(4), 461-469.

Raynolds, M.K., Walker, D.A., Maier, H.A. (2006) Alaska arctic tundra vegetation map. U.S. Fish and Wildlife Service: Anchorage, AK.

Reschke, J., Bartsch, A., Schlaffer, S., Schepaschenko, D. (2012) Capability of C-band SAR for operational wetland monitoring at high latitudes. Remote Sensing, 4(10), 2923-2943.

Rocha, A. V., Loranty, M. M., Higuera, P. E., Mack, M. C., Hu, F. S., Jones, B. M., Breen, A.L., Rastetter, E.B., Goetz, S.J., Shaver, G. R. (2012) The footprint of Alaskan tundra fires during the past half-century: implications for surface properties and radiative forcing. Environmental Research Letters, 7(4), 044039.

Soja, A. J., Tchebakova, N. M., French, N. H., Flannigan, M. D., Shugart, H. H., Stocks, B. J., Sukhinin, A.I., Parfenova, E.I., Chapin III, F.S., Stackhouse Jr, P. W. (2007) Climate-induced boreal forest change: predictions versus current observations. Global and Planetary Change, 56(3-4), 274-296.

Swanson, D. K. (1996) Susceptibility of permafrost soils to deep thaw after forest fires in interior Alaska, USA, and some ecologic implications. Arctic and Alpine Research, 28(2), 217-227.

Tape, K. E. N., Sturm, M., Racine, C. (2006) The evidence for shrub expansion in Northern Alaska and the Pan-Arctic. Global Change Biology, 12(4), 686-702.

Wein, R. W., Bliss, L. C. (1973) Changes in arctic Eriophorum tussock communities following fire. Ecology, 54(4), 845-852.

Chapter IV

Determination of Synthetic Aperture Radar Backscatter in the Tundra as a Function of Fire and Biophysical Parameters

Introduction

Wildfire effects the tundra landscape through a variety of direct and indirect mechanisms. The effects of wildfire on the tundra including changes to soil active layer thickness (ALT), soil temperature, soil moisture, depth of organic soil, and vegetation composition, structure, and abundance are well documented in the scientific literature (Liljedahl et al. 2007, Racine et al. 2004, and many others). However, the full extent and cause of variation in response to fire across the tundra are poorly documented. This is largely due to the logistical challenge of obtaining in-situ field measurements, especially repeated measurements, in remote locations. Although an impressive amount of work has been done on a few very large fire events (mostly in the single 2007 Anaktuvuk River Fire), these constitute a relatively small proportion of the fire events in Alaskan tundra (French et al. 2015). Comparatively little is known about long-term effects of smaller fire events or repeated burning in Alaskan tundra.

Fire in the Arctic tundra is generally uncommon -- especially when compared to the neighboring boreal ecoregion (Racine et al. 1985; Rocha et al. 2012, French et al. 2015). In the Alaskan tundra fire data record, small fires (~10 km^2) are significantly more common than large fires (>300 km^2). Most Arctic tundra fires begin in the months of June and July as the result of lightning ignitions (French et al. 2015).

A fire event directly impacts the landscape through combustion and removal of vegetation and organic soil. This changes the surface energy balance through a marked decrease in albedo and substantial increase in surface shortwave forcing that initiates years of impact (French et al. 2015, Rocha et al. 2012, Rocha and Shaver 2011). The surface energy balance is further compromised through reductions of the organic soil layer and the removal of vegetation, especially moss, both of which provide insulation of the permafrost. Post-fire vegetation recovery is quick, but is dominated by sedge recovery while sphagnum moss is slow to recover and the overall structure and composition of vegetation post fire can be significantly different than pre-fire conditions (Racine et al. 2004).

Studies focusing on field measurements of biophysical variables pre and post fire have shown increased soil moisture, increased soil temperature, increased active layer thickness (depth of seasonal soil thaw), and earlier onset of frozen ground in the fall post fire in addition to changes in vegetation (Liljedahl et al. 2007, Mackay 1995, Racine et al. 2004, Tsuyuzaki et al. 2018, Wein and Bliss 1973).

From the high-severity, large Anaktuvak River Fire the scientific community has obtained data points and observations for the upper range of intense tundra fire conditions.

The Anaktuvak River Fire is the largest fire on record (1,039 km^2 burned) for the tundra biome and doubled the cumulative area burned north of 68°N since 1950 (Hu et al. 2010). The Anaktuvak River Fire appears to be a novel expression in the tundra fire record with a late-season, September-October burn and greater burn severity than typical tundra fire resulting from a large temperature anomaly (Jones et al. 2009). Alternatively, this fire may represent the new normal (Hu et al. 2010). Some have speculated that tundra fires may be better indicators of climate change than boreal fires because occurrence is even more predicated on climate than fuel (Racine and Jandt, 2008).

Wildfire is a climate-sensitive process. Measurements from the Anaktuvuk River Fire show the upward potential for large quantities of carbon release from a large and severe tundra fire. Recent observations indicate increased burned area in the tundra over the past two decades (Higuera et al. 2008, Hu et al. 2010). Given changes in climate, tundra fires could become both more frequent and severe in the future (Hu et al. 2010). Increasing fire in the Arctic could rapidly transfer large amounts of carbon to the atmosphere, reduce landscape carbon storage, and amplify climate warming through increased levels and post-fire changes to the ecosystem.

A transition to a shrub-dominated system and an associated reduction in lichen and moss cover has been observed across the Arctic and has significantly changed plant community structure in some areas (Fraser et al. 2014, Tape et al. 2006, Myers-Smith et al. 2011, Lantz et al. 2013, Ropars and Boudreau 2012, Tremblay et al., 2012). Shrub expansion is attributed to temperature increases that have directly removed limitations to reproduction and growth (Walker 1987, Lantz et al. 2010). Indirectly increased soil microbial activity and mobilization of

limiting nutrients has also resulted in increased shrub cover (Strum et al. 2005). Vegetation is the fuel that sustains fire, and through an increase in woody vegetation from increased shrub cover fuel reserves are expected to increase over time (Chapin et al. 2005, Tape et al. 2006). These enhanced fuel reserves could potentially result in increased areas burned and fire severities. The possibility for positive feedback mechanisms also exist as shrub cover has been found to be higher in fire-affected areas (Racine et al. 2004).

While much is known about the modern fire data record in the tundra, starting with the 1950s, there are likely many omissions (French et al. 2015). Methodologies for fire detection and mapping include satellite technologies, but typical tundra fires are small with duration on the order of days. Fine-scale spatial resolution satellite systems are only available as recent as the early 1970s, and persistent cloud cover in the Arctic limits usable pixels within the short growing season widow of available images. Furthermore, recent research (Loboda et al. 2013) using electro-optical satellite images shows the spectral signature of burned areas in the tundra deteriorate rapidly, and are potentially poorly distinguishable by the end of the first post-fire season. Using microwave synthetic aperture radar (SAR) data fire scars are distinguishable longer (4-5 years) than can be observed with electro-optical images (Jenkins et al. 2014). Microwave data also provide the added benefit of more look images due to all-weather images capabilities, but image interpretation and understanding of the physics governing SAR image formation are more complex.

The goal of this study is to better understand the SAR signal, or “backscatter”, in burned areas of Arctic tundra in order to develop more tools for post-fire effects characterization at the landscape and regional scale. The objective is to parameterize a preliminary model to link SAR

satellite data to a suite of in-situ biophysical variables. Microwave data provide a means to go beyond the limitations of electro-optical satellite systems by providing information on the vegetation structure, biomass, and moisture conditions. By looking at a rich dataset of different biophysical parameters measured in different fire histories, time since fire, and repeated versus single burning we can we better characterize and understand the microwave remote sensing signal post-fire.

Materials and Methods

Field Data

We made field observations in the Alaskan tundra in August of each year for three years (2016-2018) in two different geographic regions -- the Noatak National Preserve and Seward Peninsula. Burned areas were determined from the Alaska Large Fire Database (https://afsmaps.blm.gov/imf/imf.jsp?site=firehistory), which provides a fire record for the region dating back to 1950. The database contains reported fire locations and fire perimeters since 1939 and 1942 respectively (Olson et al. 2011), but records were not systematically kept until the 1950s.

In the present study, the timing of field data collection was focused on maximizing active layer thickness from seasonal permafrost melt while still capturing robust vegetation conditions prior to seasonal senescence. We collected field data in August of each year to measure late-season conditions while still maintaining favorable weather conditions.

Our fire scar field sites were selected based on accessibility for the field team, including proximity to road and river networks. We accessed fire scars in the Noatak National Preserve on foot from the Noatak River. We accessed fire scars in the Seward Peninsula on foot from the road network. Within a fire scar, a stratified random sampling approach was used to select site location. Sites were stratified by burn severity and selection was limited to within a buffer from the road or river network of 3 km. Unburned sites with no known fire history since 1950 were also randomly selected within cover types that were representative of burned tundra. Site locations were determined randomly on a digital map, after which the field team walked or drove to each location. A summary of the field data collected by year and site type is shown in Table 1. A total of 171 burned data plots and 25 unburned plots were obtained over the three-year period. Data have been collected in 24 total named fires (Table 2). Maps showing the location of the field points are shown in Figure 4-1.

Table 4-1. *Summary of field data collected by sampling year and field site type*

	2016	**2017**	**2018**	**SUM**
Burn Plots	72	60	39	171
Unburned Plots	9	11	5	25
Active Layer Thickness Sites	338	159	161	658
SUM	419	230	205	854

Table 4-2. *Summary of named fires sampled by year. For each fire, the year it occurred is given in parentheses.*

2016	**2017**	**2018**
NOA (1971) Noatak River (2014) WTK N 60 (1984) Goiter Fire (2005) Kaluktavik River (2010) Sisiak Creek (2004) Uchugrak Hills (2000) IAN N 55 (1984) Uyon Lakes (2003) Uyon Lakes (2012) N Noatak (1976) AVAN (1972)	Imuruk Basin (1954) Cairn 4 (1971) Mingvk Lake (2015) Milepost 85 (2002) Delome River (1971) ANC NW 500 (1971) Garfield Creek (1997)	Makpik Creek (2010) OTZ NE 100 (1985) Cottonwood Bar (2002) IAN N 63 (1983) Aklummayuak (2005)
SUM: 12	7	5
TOTAL: 24		

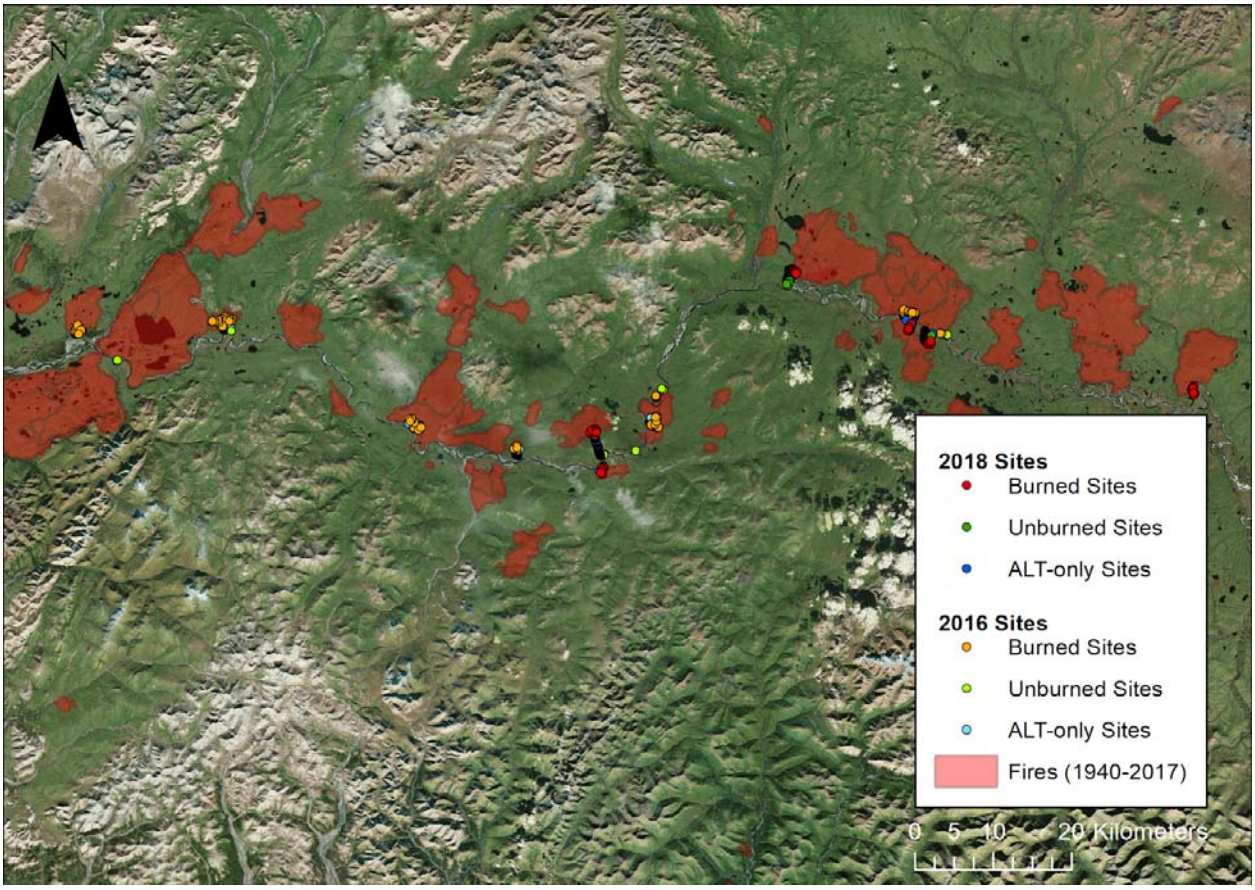
N
2018 Sites
Burned Sites
Unburned Sites
ALT-only Sites
2016 Sites
Burned Sites
Unburned Sites
ALT-only Sites
Fires (1940-2017)
0 5 10 20 Kilometers

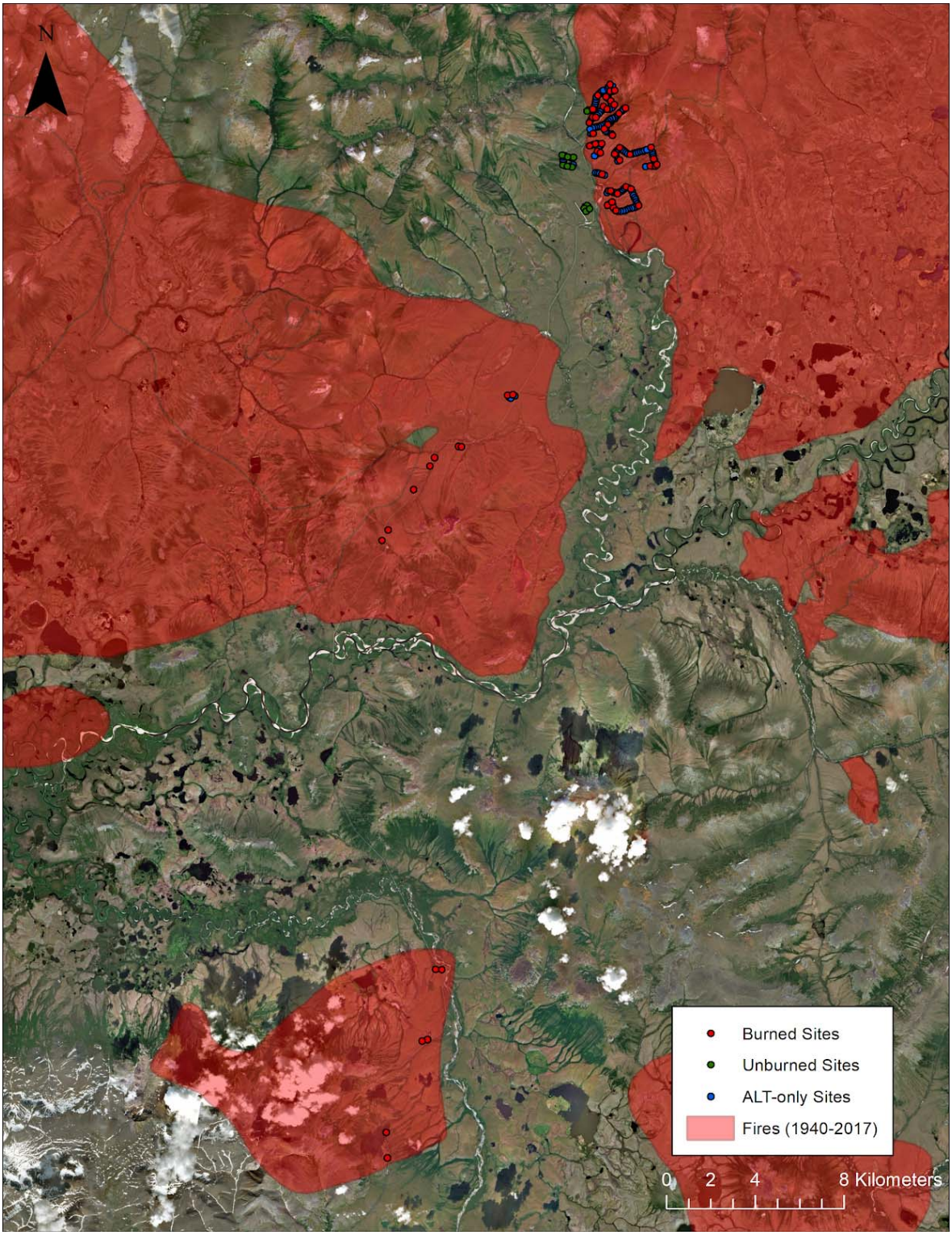

Figure 4-1. *Data have been collected in the Noatak River Valley in 2016 and 2018 (top) and the Seward Peninsula in 2017 (bottom). Red points represent burned sites, green unburned sites, and blue where only Active Layer Thickness (ALT) and soil temperature have been measured.*

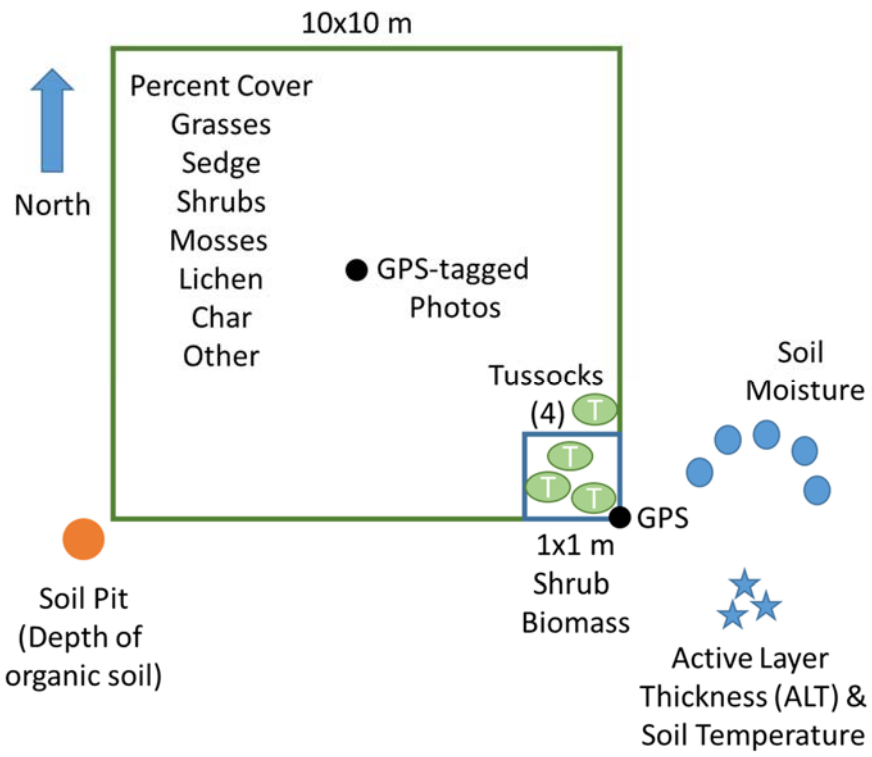

Figure 4-2. *At each site a suite of biophysical parameters were measured.*

A suite a biophysical parameters were measured at each field site (Figure 4-2). A 10x10m field plot was used to obtain percent ground cover of moss, lichen, grasses, sedges, shrubs, char, and other summing to 100 percent. A smaller 1x1m field subplot, within the corner of each 10x10m field plot, was used to measure shrub biomass. The diameter of each shrub within the 1x1m field subplot was measured using Vernier calipers and average height of all shrubs above the ground surface was recorded. The four closest tussocks to the plot outermost corner and within the 1x1m field subplot were measured. The length, width, and depth of each tussock were recorded as well as the distance from the cornermost tussock to the next three tussocks. At the plot corner, GPS data of latitude and longitude were measured. Also at the plot corner, three replicates of ALT and soil temperature were measured. ALT was

measured using a steel rod inserted into the soil from the surface and pressed downward until hitting a frozen soil layer. Adjacent to the ALT measurements, five replicates of soil moisture at 6cm depth and five replicates of soil moisture at 12cm depth were measured using a Campbell Scientific Hydrosense II handheld soil moisture probe. At the adjacent corner of the 10x10m plot a soil pit was excavated to measure depth to mineral soil with 3 replicate measurements within the pit. Additional site information included: site name, date, time, GPS location, GPS-tagged photos in each cardinal direction and nadir (straight down from chest height), site description, and current and previous 12-hour weather conditions, if known.

Stem diameters for all individual shrubs in the 1x1m vegetation subplot were converted to biomass using allometric equations derived at the U.S. Forest Service (Smit and Brand, 1983). As described in the allometric equation methodology, all basal diameters were measured at stem base except bog birch (*Betula pumila*) which was measured at 15 cm from ground. Biomass was calculated as grams per square meter as a function of contributions from *Betula pumila*, *Salix spp.*, *Rhododendron groenlandicum*, *Vaccinium uliginosum*, *Dasiphora fruticosa*, *Picea spp.*, *Alnus viridis*, *Alnus spp.*, and *Rhododendron lapponicum*.

Tussock length and width measurements were used to calculate compacted and uncompacted area of each tussock. Area of the four tussocks were averaged to determine an average area per site. Assuming a tussock is well represented as an ellipse, the following equation was used:

Tussock area = π * tussock length * tussock width

The percent Volumetric Moisture Content (%VMC) as reported by the Campbell Scientific Hydrosense handheld soil moisture probes is based on a loam mineral soil. Organic soils found in the tundra have a characteristic low bulk density and the default loam calibration typically underestimates actual soil moisture condition. To develop a calibration for organic soils in the tundra eight soil samples were extracted from the Noatak National Preserve and the Seward Peninsula to use in a laboratory setting to develop gravimetric based calibration algorithms (Bourgeau-Chavez et al. 2010). Soil samples were collected in burned and non-burned tundra. The best calibration curves were found by combining all 8 samples with 13 additional tundra samples from the North Slope of Alaska to develop an overall tundra calibration.

The equation for calibrated %VMC is:

$\theta = A * \tau 2 + B * \tau + C$

Where:

θ = VMC

τ = Probe Period

With coefficients A, B, and C as follows:

	Probe Length	A	B	C	RSME
HydroSense I	20 cm	-7.63	142.74	-102.96	4.115
HydroSense I	12 cm	-191.26	523.66	-284.08	12.988
HydroSense I	6 cm	-314.98	761.32	-388.77	13.591
HydroSense II	20 cm	12.14	-14.31	-0.81	4.803
HydroSense II	12 cm	-18.78	124.47	-106.93	12.129
HydroSense II	6 cm	-3.93	61.09	-32.88	9.781

Field data and derived biophysical calculations will be archived and published at the ORNL DAAC (https://daac.ornl.gov/). The ORNL DAAC is sponsored by NASA and serve as the primary active archive for biogeochemical dynamics data derived from NASA's field campaigns, including the Arctic-Boreal Vulnerability Experiment (ABoVE) under which this field data were collected.

Remote Sensing Data

From SAR theory we know backscatter is a function of frequency, polarization, incident angle, dielectric constant (moisture), and surface roughness. Frequency, polarization, and incident angle are all determined by SAR sensor and system configuration details, whereas moisture and surface roughness are dictated by microwave signal interactions with ground cover. Fire events affect the SAR signature through an approximately 3 dB increase in backscatter in recently burned areas which persists 4-5 years (Jenkins et al. 2014). I and colleagues hypothesized that the increase in backscatter post-fire is the result of changes in moisture conditions (Jenkins et al. 2014).

We therefore expect backscatter in the tundra to be a function of fire occurrence, moisture, and surface roughness (Figure 4-3). Surface roughness is predicted based on the wavelength of the SAR sensor. Surface roughness has been discussed in the tundra fire literature, but it has been in terms of energy flux and atmospheric dynamics (Liljedahl et al. 2007, Rocha and Shaver 2011, Chambers and Chapin 2003, Jones et al. 2015). Despite different applications, these discussions are relevant to determining surface roughness contributions to SAR backscatter. In the low-biomass treeless tundra potential contributions to the surface roughness signal could result from shrubs and tussocks, and the configuration of these on the landscape, in addition to microtopography from permafrost features. Liljedahl et al. (2007) measured a doubling of the surface roughness coefficient from severe combustion of moss essentially increasing the height of tussocks. Jones et al. (2015) measured a 340% increase of rugosity, or surface roughness, from the degradation of ice wedges post fire in the Anaktuvuk River Fire.

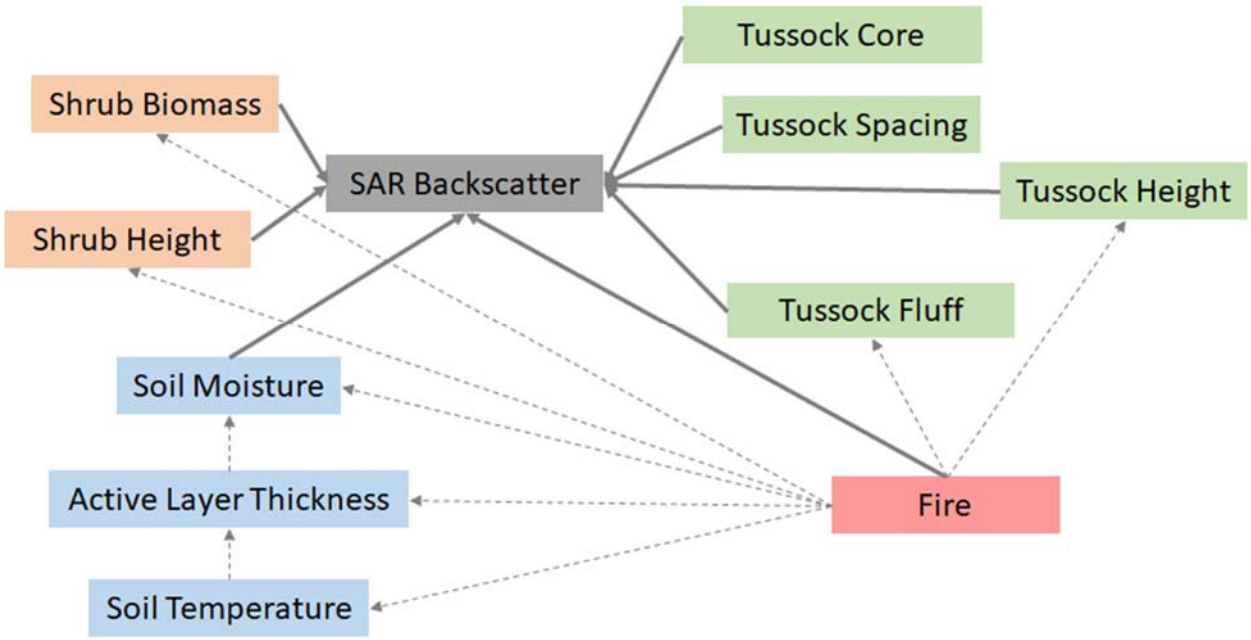

Figure 4-3. *In the tundra we expect SAR backscatter to result from a function of contributions from shrubs (orange), tussocks (green), moisture (blue), and fire (red). Direct contributions to backscatter are indicated with a solid grey line. Indirect contributions are shown by a dashed grey line.*

Sentinel-1A and 1B C-band satellite synthetic aperture radar data were used in this study. Satellite images closest to the day of field data collection for a given field site were used. Temporal offset from date of field data collection to satellite image date ranged from 0 to 17, with an average of 7 days. SAR images were processed within GoogleEarth Engine. GoogleEarth Engine data are pre-processed using the Sentinel-1 Toolbox to conduct thermal noise removal, radiometric calibration, and terrain correction using ASTER DEM. A 3x3 mean image filter was applied to all study images. Interpolated incidence angle data are available by pixel and ranged from 30 to 45 degrees for the study sites. Pixel values in intensity were converted to dB using the following equation:

$dB = 10*\log_{10}(intensity)$

Burn severity was determined using the Landsat data record. Tasseled Cap Greenness and Brightness and single Landsat bands (near-infrared) were used to map burn severity as these methods are found to be superior to detecting severity in the tundra over common mapping methods based on the normalized burn ratio (Loboda et al. 2013). Severity was mapped using burn severity index (BSI) values 0 through 4, with 0 representing unburned tundra and 1 low severity through 4 high severity.

Statistical Analysis

A series of linear models were developed for this study. All models were developed in R (R Core Team, 2013) using the lm() function. Linear models were developed to model backscatter as a function of the biophysical field parameters. After testing whether biophysical variables could be used to model SAR backscatter across the full range of site fire histories, and

finding that they could not, data were stratified into seven groups with similar time since last fire periods (years) and modeled independently.

Based on my conceptual model of backscatter (Figure 4-3) the in-situ field variables were grouped by category (moisture condition, shrubs, tussocks, and fire). The moisture variables include soil moisture at 6 cm depth, active layer depth, and soil temperature. The shrub variables include shrub biomass, shrub height, and shrub percent cover. The tussock variables include the area of uncompacted tussock, the area of tussock core, tussock height, and distance between tussocks or tussock spacing. The fire variables include fire count and year since fire.

Results

No one statistically significant model was found for all of the sites. However, by grouping sites with similar fire histories relationships between backscatter and biophysical variables emerged (Table 4-3). The best models were for recently burned tundra (2-4 years post fire, $R^2 = 0.464$), fires 15-16 years post fire ($R^2 = 0.554$), and unburned tundra ($R^2 = 0.508$). The fire grouping of 6 and 8 years post fire were marginally significant with a p-value of 0.086. No statistically significant models were found for the grouping of 32, 33, and 35 years post fire. Approximately a third to a half of the variation in backscatter among field sites examined was explained by these model variables across the entire dataset (adjusted R-squared ranging from 0.311 to 0.554). Models were developed for VH backscatter as better relationship were found using VH as opposed to VV in the Sentinel-1 data.

The statistical models suggested that backscatter in the tundra was primarily related to moisture condition, shrub characteristics, tussock characteristics, and fire history.

Table 4-3. *Results of modelling VH backscatter as a function of moisture condition (blue), shrubs (orange), tussocks (green), and fire (red).*

Year since fire	n=1	p-value	adj R	Soil moisture 6 cm	Active Layer Depth	Soil Temp	Shrub Biomass	Shrub Height	Shrub Percent Cover	Tussock Fluff Area	Tussock Core Area	Tussock Height	Tussock Spacing	Fire Count	Year Since Fire
Unburned	24	0.032	0.508	0.317			0.018 *			0.03881 *	0.086	0.037 *	0.004 **	NA	NA
45, 46	20	0.017	0.3619								0.074			0.008 **	
32, 33, 35	27														
15,16	38	0.008	0.554	0.09		0.021 *	0.106	0.099			0.086	0.002 **	0.031 *	0.002 **	
11,12,13	30	0.026	0.311	0.092					0.063		0.041 *	0.135			0.015 *
6,8	16	0.086	0.309		0.07			0.158		0.1536					
2,4	37	0.003	0.464	0.040*	0.031 *		0.066	0.034 *		0.003 **	0.012 *				0.036*

Discussion

The range of observed values of the various field parameters across the field sites were large and the correlations between backscatter and the individual biophysical variables that we measured were relatively low. There were also issues associated with the SAR data and spatial averaging to reduce effects of speckle that dilute the signal. Nonetheless, the models confirm much of our theoretical understanding of backscatter and provide the basic information needed to further refine techniques and develop more robust interpretive models.

The model results suggest contributions from active layer depth and soil temperature in the subsurface, which do not directly affect backscatter as measured by SAR. The C-band SAR signal is not penetrating the organic soil column to the depth of seasonal thaw. The significance of these variables must be the result of indirect contributions to backscatter (see Figure 4-1). Soil moisture can vary on a shorter time scale than the other parameters in the model, but the assumption here is that the field measured soil moisture at 6 cm is representative of overall site moisture condition. The Arctic tundra is characterized by low precipitation, with less than 10 inches per year, making the tundra a desert-like climate.

SAR is a coherent sensor and images contains speckle that introduces variance into the image intensity or radar backscatter. To account for this inherent noise, SAR images are filtered, or averaged. In this study a three by three mean average filter was used, essentially increasing the ground covered by a pixel from 10x10m to 30x30m. This works against correlations of backscatter to field biophysical parameters in two ways: 1) it dilutes the signal;

and 2) it introduces more ground cover variation since a larger area of ground is represented in the pixel value.

Sentinel data was extracted using GoogleEarth Engine. The use of GoogleEarth Engine significantly reduced SAR processing time, but data are terrain corrected using an ASTER DEM north of 60 degrees latitude. This is not the best digital elevation model for the region, which may reduce geocoding accuracy, especially in mountainous areas.

SAR data used in this study are C-band Sentinel. Other SAR platforms exist and could be used to investigate the relationship at different wavelengths or incident angles. Sentinel data contain contains information on incident angle by pixel. The range of incident angles across the field sites are 30-45 degrees. There are methods to account for differences in incident angle and to correct for incident angle effects that may improve relationships (Abbott et al. 2007).

The next step is to disentangle the contributions of moisture condition, shrub characteristics, tussock characteristics, and fire history to backscatter. This could be accomplished through polarimetric SAR data and the use of polarimetric decompositions similar to what has been done in the boreal forest (Bourgeau-Chavez et al. 2013). Additionally, causal inference and machine learning techniques such as structural equation modelling and might prove useful.

Conclusions

We showed that a significant proportion of variability in SAR backscatter observations in the tundra of Alaska can be modeled statistically as function of the variability in moisture condition, shrubs, tussocks, and fire history, each characterized at the site scale. Contributions

of different biophysical variables to the backscatter signal vary as a result of year since fire, but models show contributions from all four categories in almost all fire histories. Fire scars are 3 dB brighter than the surrounding landscape in the 4-5 years immediately preceding fire (Jenkins et al. 2014), but this change in backscatter does not appear to be primarily or solely driven by moisture condition as previously thought. Shrubs and tussocks are also shown to be important contributors.

The next step is to disentangle the contributions of moisture condition, shrubs, tussocks, and fire to backscatter. This could be accomplished using polarimetric SAR data and polarimetric decomposition. Laboratory testing of tussocks could also be useful for determining scattering mechanisms and the contributions of the uncompacted tussock versus the core and tussock height and tussock spacing.

SAR is a powerful tool for monitoring in the Arctic where persistent cloud cover and haze affect electro-optical systems. SAR data also go beyond the data obtainable in electro-optical systems and provide information on the vegetation structure, biomass, and moisture conditions. Once we have determined the contributions to backscatter in the tundra we can use SAR to better detect fires, monitor fire recovery, and measure fire effects at the regional and landscape scale. Given limited human habitation in the region and the challenges of accessing remote area of the tundra, we need these cutting-edge tools and techniques to monitor from afar.

References

Abbott, K. N., B. Leblon, G. C. Staples, D. A. Maclean, and M. E. Alexander (2007) Fire danger monitoring using RADARSAT-1 over northern boreal forests. International Journal of Remote Sensing 28, no. 6: 1317-1338.

Bourgeau-Chavez, L. L., Leblon, B., Charbonneau, F., Buckley, J. R. (2013) Evaluation of polarimetric Radarsat-2 SAR data for development of soil moisture retrieval algorithms over a chronosequence of black spruce boreal forests. Remote Sensing of Environment, 132, 71-85.

Bourgeau-Chavez, L.L., Garwood, G.C., Riordan, K., Koziol, B.W., and Slawski, J. (2010) Calibration algorithm development for selected water content reflectometers to burned and non-burned organic soils of Alaska. International Journal of Wildland Fire, Vol. 19:961-975.

Chambers, S. D., Chapin, F. S. (2002) Fire effects on surface-atmosphere energy exchange in Alaskan black spruce ecosystems: Implications for feedbacks to regional climate. Journal of Geophysical Research: Atmospheres, 107(D1).

Chapin, F.S., Sturm, M., Serreze, M.C., McFadden, J.P., Key, J.R., Lloyd, A.H., McGuire, A.D., Rupp, T.S., Lynch, A.H., Schimel, J.P., Beringer, J. (2005) Role of land-surface changes in Arctic summer warming. Science, 310(5748), 657-660.

Fraser, R. H., Lantz, T. C., Olthof, I., Kokelj, S. V., Sims, R. A. (2014) Warming-induced shrub expansion and lichen decline in the Western Canadian Arctic. Ecosystems, 17(7), 1151-1168.

French, N.H.F., M.A. Whitley and L.K. Jenkins (2016) Fire disturbance effects on land surface albedo in Alaskan tundra. J. Geophysical Research, 121(3): 841-854 DOI: 10.1002/2015JG003177

French, N. H. F., L. K. Jenkins, T. V. Loboda, M. Flannigan, R. Jandt, L. L. Bourgeau-Chavez, and M. Whitley (2015) Fire in arctic tundra of Alaska: past fire activity, future fire potential, and significance for land management and ecology. Int. J. Wildland Fire, http://dx.doi.org/10.1071/WF14167

Higuera, P. E., Brubaker, L. B., Anderson, P. M., Brown, T. A., Kennedy, A. T., Hu, F. S. (2008) Frequent fires in ancient shrub tundra: implications of paleorecords for arctic environmental change. PLoS One, 3(3), e0001744.

Hu, F. S., Higuera, P. E., Walsh, J. E., Chapman, W. L., Duffy, P. A., Brubaker, L. B., Chipman, M. L. (2010) Tundra burning in Alaska: linkages to climatic change and sea ice retreat. Journal of Geophysical Research: Biogeosciences (2005–2012), 115(G4).

Jones, B. M., Grosse, G., Arp, C. D., Miller, E., Liu, L., Hayes, D. J., Larsen, C. F. (2015) Recent Arctic tundra fire initiates widespread thermokarst development. Scientific Reports, 5, 15865.

Jenkins, L.K., Bourgeau-Chavez, L.L.; French, N.H.F., Loboda, T.V., Thelen, B.J. (2014) Development of Methods for Detection and Monitoring of Fire Disturbance in the Alaskan Tundra Using a Two-Decade Long Record of Synthetic Aperture Radar Satellite Images. Remote Sens. 6, no. 7: 6347-6364.

Lantz, T. C., Gergel, S. E., Kokelj, S. V. (2010) Spatial heterogeneity in the shrub tundra ecotone in the Mackenzie Delta Region, Northwest Territories: implications for Arctic environmental change. Ecosystems, 13(2), 194-204.

Liljedahl, A., Hinzman, L., Busey, R., Yoshikawa, K. (2007) Physical short-term changes after a tussock tundra fire, Seward Peninsula, Alaska. Journal of Geophysical Research: Earth Surface, 112(F2).

Loboda, T. V., French, N. H. F., Hight-Harf, C., Jenkins, L., Miller, M. E. (2013) Mapping fire extent and burn severity in Alaskan tussock tundra: An analysis of the spectral response of tundra vegetation to wildland fire. Remote Sensing of Environment, 134, 194-209.

Mackay, J. R., (1995) Active layer changes (1968 to 1993) following the forest-tundra fire near Inuvik, N.W.T., Canada. Arctic and Alpine Research, 27(4): 323–336.

Masrur, A., Petrov, A. N., DeGroote, J. (2018) Circumpolar spatio-temporal patterns and contributing climatic factors of wildfire activity in the Arctic tundra from 2001–2015. Environmental Research Letters, 13(1), 014019.

Michaelides, R., Schaefer, K., Zebker, H., Parsekian, A., Liu, L., Chen, J., Natali, S.M., Ludwig, S., Schaefer, S. (2018) Inference of the impact of wildfire on permafrost and active layer thickness in a discontinuous permafrost region using the remotely sensed active layer thickness (ReSALT) algorithm. Environmental Research Letters.

Myers-Smith, I. H., Forbes, B. C., Wilmking, M., Hallinger, M., Lantz, T., Blok, D., Tape, K.D., Macias-Fauria, M., Sass-Klaassen, U., Lévesque, E., Boudreau, S. (2011) Shrub expansion in tundra ecosystems: dynamics, impacts and research priorities. Environmental Research Letters, 6(4), 045509.

Olson D.L., Cronan J.B., McKenzie D., Barnes J.L., Camp A.E. (2011) Compiling, synthesizing, and analyzing existing boreal forest fire history data in Alaska. Joint Fire Science Program Project no. 06-3-1-26. Available at https://www.firescience.gov/projects/06-3-1-26/project/06-3-1-26_final_report.pdf

Racine, C., Jandt, R. (2008) The 2007 ‘Anaktuvuk River’tundra fire on the Arctic Slope of Alaska: A new phenomenon. In Ninth International Conference on Permafrost, US Permafrost Assoc., Fairbanks, Alaska (Vol. 29).

Racine, C., Jandt, R., Meyers, C., Dennis, J. (2004) Tundra fire and vegetation change along a hillslope on the Seward Peninsula, Alaska, USA. Arctic, Antarctic, and Alpine Research, 36(1), 1-10.

Racine, C. H., Dennis, J. G., Patterson III, W. A. (1985) Tundra fire regimes in the Noatak River watershed, Alaska: 1956-83. Arctic, 194-200.

Rocha, A. V., Loranty, M. M., Higuera, P. E., Mack, M. C., Hu, F. S., Jones, B. M., Breen, A.L., Rastetter, E.B., Goetz, S.J., Shaver, G.R. (2012) The footprint of Alaskan tundra fires during the past half-century: implications for surface properties and radiative forcing. Environmental Research Letters, 7(4), 044039.

Rocha, A. V., Shaver, G. R. (2011) Postfire energy exchange in arctic tundra: the importance and climatic implications of burn severity. Global Change Biology, 17(9), 2831-2841.

Ropars, P., Boudreau, S. (2012) Shrub expansion at the forest–tundra ecotone: spatial heterogeneity linked to local topography. Environmental Research Letters, 7(1), 015501.

R Core Team (2013) R: A language and environment for statistical computing. R Foundation for Statistical Computing, Vienna, Austria. URL http://www.R-project.org/.

Smith, W. B., Brand, G. J. (1983) Allometric biomass equations for 98 species of herbs, shrubs, and small trees. Research Note NC-299. St. Paul, MN: US Dept. of Agriculture, Forest Service, North Central Forest Experiment Station, 299.

Sturm, M., Schimel, J., Michaelson, G., Welker, J.M., Oberbauer, S.F., Liston, G.E., Fahnestock, J., Romanovsky, V. E. (2005) Winter biological processes could help convert arctic tundra to shrubland. Bioscience, 55(1), 17-26.

Tape, K. E. N., Sturm, M., Racine, C. (2006) The evidence for shrub expansion in Northern Alaska and the Pan-Arctic. Global Change Biology, 12(4), 686-702.

Tremblay, B., Lévesque, E., Boudreau, S. (2012) Recent expansion of erect shrubs in the Low Arctic: evidence from Eastern Nunavik. Environmental Research Letters, 7(3), 035501.

Tsuyuzaki, S., Iwahana, G., Saito, K. (2018) Tundra fire alters vegetation patterns more than the resultant thermokarst. Polar Biology, 41(4), 753-761.

Wein, R. W., Bliss, L. C. (1973) Changes in arctic Eriophorum tussock communities following fire. Ecology, 54(4), 845-852.

Zwieback, S., Berg, A. A. (2019) Fine-Scale SAR Soil Moisture Estimation in the Subarctic Tundra. IEEE Transactions on Geoscience and Remote Sensing.

Chapter V

Conclusions

Climate change is accelerated in the Arctic and rapid changes are occurring in terrestrial and marine environments. Widespread transformations are occurring in ecosystem structure and function with significant implications for natural and human systems. Global-scale climate forcing can be expected to affect regional-scale disturbances, which in turn may affect socio-economic conditions at local to global scales. Both the natural, terrestrial and marine environments of the Arctic and people that depend on the region's resources face an uncertain future in terms of environmental conditions and sustainability of ecosystem services.

Scientific data are needed for informed decision-making and to guide societal response to climate change. Data are also needed to improve analysis and modelling capabilities in order to better understand and predict ecosystem response to change. The Arctic environment is complex and data are needed across a variety of disciplines and domains to match the observed interdependencies and feedbacks.

The collection and analysis of remotely sensed data are needed to study the Arctic and constitute a key element of the path forward. Satellite remote sensing provides synoptic datasets that may be the first line of defense in detection of change. Advanced data analysis

methodologies are needed to separate real change from natural variability and to detect departures from steady state at a variety of temporal scales.

Through my dissertation research I found that standardizing in terms of data and satellite platform provides an unbiased comparison across numerous disparate variables and across terrestrial (land surface) and marine (sea surface) environments and provides a method to detect and evaluate environmental change. Significant temporal trends were found in almost all observed variables over the 18-year period. Analysis of seasonal data revealed significant breakpoints in temporal trends. Within the terrestrial environment, data showed significant increasing trends in land surface temperature and NDVI. In the marine environment, significant increasing trends were detected in primary productivity. Significantly earlier onset of green up date was observed in bioclimate subzones C&E and longer end of growing season in B&E. Terrestrial and marine observations show similar rates of change with unidirectional change in terrestrial and significant directional and magnitude shifts in marine.

MODIS is a powerful monitoring and analysis tool for the Arctic in terms of spatial coverage of the entire pan-Arctic on a daily timescale. The growing season in the Arctic is short and the temporal resolution afforded by MODIS is needed in order to capture phenological and seasonal changes occurring on a daily to weekly scale. Having daily data also provides a means to account for cloud cover in the Arctic through composite images.

The dissertation research that focused on Synthetic Aperture Radar (SAR) showed that SAR is a powerful tool for use in the Arctic where significant cloud cover and haze affect electro-optical image acquisition. I found that SAR data not only provided more images within the short Arctic growing season due to all-weather imaging, but SAR readily detected burned

areas in the tundra with a doubling of the satellite signal (3 db). I further found that burned areas in the tundra are detectable in the SAR satellite data record for many more years than in the electro-optical record (four to five years instead of one).

By looking at a rich dataset of in-situ variables and developing a conceptual model of SAR backscatter in the tundra, I found that a significant proportion of variability in SAR backscatter observations in the Alaskan tundra can be modeled statistically as function of the variability in moisture condition, shrubs, tussocks, and fire history, each characterized at the site scale. Contributions of different biophysical variables to the backscatter signal varied as a result of year since fire, but models showed contributions from all four categories in almost all fire histories. This showed that SAR data is sensitive to a larger set of variables (vegetation structure, biomass, and moisture conditions) than electro-optical (vegetation greenness and composition/type) data and can be used to monitor a different set of trajectories of change and recovery post-fire.

Remotely sensed data needs to be informed by on-the-ground data and understanding of processes occurring at different scales. With increased access to remote sensing data and increased data streams we are at risk to conducting data analysis entirely from afar as there is no limit to the volume of data and the models we can develop to utilize these data streams. The scientific community needs to work with local residents and spend time in the areas we are studying in order to understand the environment, the connections, and subtle nuances that may be a key component to the overall understanding of the system.